Geological Quarterly, Vol. 40, No. 3, 1996, p. 407–442

Stanisław Z. MIKULSKI

Gold mineralization within contact-metamorphic and shear zones in the "Złoty Jar" quarry — the Złoty Stok As-Au deposit area (Sudetes)

Mineral paragenesis of gold mineralization in the "Złoty Jar" quarry has been formed during three separated stages. The stage I of skarn-like mineralization was due to metasomatic processes developed in the exocontact zone of the Variscan Kłodzko – Złoty Stok granodiorite massif. Preliminary results of primary fluid inclusion studies demonstrate that the earliest stage with pyroxene, garnet and scheelite have low salinity fluids (4.9–5.2 wt. % NaCl equiv.) at temperatures between 464–480°C and pressure below 1.4 kbar. During later phases of this stage widespread gold-bearing ore mineralizations (loellingite, arsenopyrite) were formed. Definitely most gold occurs as fine-dispersed submicroscopic particles within ore minerals in calc-silicate and black serpentinite rocks (up to 10 and 29 g/t, respectively). Younger gold-bearing stages (II and III) revealed a succession of cycles of brittle deformation and hydrothermal infill of mineralizing fluids connected with development of shear zones. Th of primary inclusions of quartz veins containing ores with native gold were determined at 220–280°C and salinity 4–10 wt. % NaCl equiv. "Visible" gold was found as inclusions from 5 to 50 μm in size among Ni-Fe-Co sulphoarsenides, sulphides and as individual micro-grains in quartz ± calcite veinlets. In the youngest described gold-bearing stage (III), inclusions of electrum and gold-bismuth myrmekites in sulphoarsenides were commonly observed. Processes of redistribution of primary gold on a local scale from loellingite-arsenopyrite mineralization, and on regional scale from metavolcanic rocks, were widely developed. Precipitation of "visible" gold within sulphoarsenides and sulphides was carried out by sulphur-bearing solutions at 350–250°C and near neutral — to alkaline environments, with dominant role of hydrosulphide complex $Au(HS)_2^-$. Main sources of metals were probably the metal preconcentrations in volcano-sedimentary rocks with mantle contribution (Pt, Pd) (?) which later underwent mobilization due to formation of granitoid intrusions and development of shear zones.

INTRODUCTION

The "Złoty Jar" (Golden Creek) quarry is located in northern part of the Góry Złote Mts. (Sudetes, SW Poland) between old mining fields of the Złoty Stok As-Au deposit (Fig. 1). The big gold rush took place between 1545 and 1549 when over 190 mining workings were

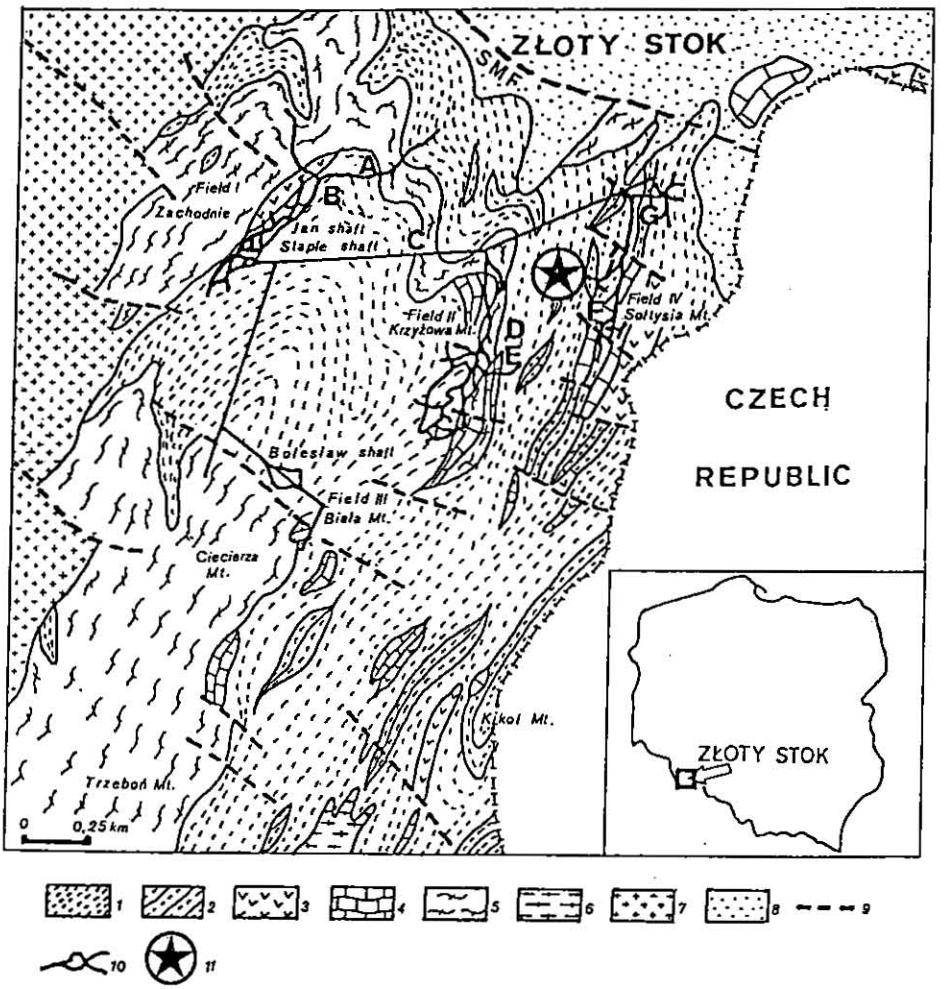

Fig. 1. Geological sketch of the study area (according to S. Cwojdziński, 1974, 1975; L. Finckh, G. Fischer, 1938; L. Sawicki, 1956) with location plan of principal workings of the Złoty Stok As-Au mine (according to the mines report, L. Bałdys, 1954) marked by the author

1 — blastomylonitic schists and biotite gneisses; 2 — streaky quartz-feldspar gneisses; 3 — amphibolites; 4 — marbles and calc-silicate rocks; 5 — Haniak gneisses; 6 — Jawornik granodiorites; 7 — Kłodzko – Złoty Stok granitoids; 8 — Quaternary sediments (undivided); 9 — faults; 10 — mine workings; 11 — the "Złoty Jar" quarry; A — Emanuela drain adit; B — Barbara gallery; C — Gertruda conveyor road; D — Krzyżowa gallery; E — Książęca gallery; F — Czarna gallery; G — Nowa gallery; SMF — Sudetic Marginal Fault

Szkic geologiczny badanego obszaru (według S. Cwojdzińskiego, 1974, 1975; L. Finckha, G. Fischera, 1938; L. Sawickiego, 1956) z planem sytuacyjnym głównych wyrobisk górniczych kopalni As-Au w Złotym Stoku (według dokumentacji kopalnianej L. Bałdysa, 1954) zaznaczonym przez autora

1 — blastomylonityczne łupki i gnejsy biotytowe; 2 — kwarcowo-skaleniowe gnejsy smugowane; 3 — amfibolity; 4 — marmury i skały wapienno-krzemianowe; 5 — gnejsy haniackie; 6 — granodioryty jawornickie; 7 — granitoidy kłodzko-złotostockie; 8 — osady czwartorzędowe (nierozdzielone); 9 — uskoki; 10 — wyrobiska kopalniane; 11 — kamieniołom „Złoty Jar"; A — szyb odwadniający Emanuela; B — sztolnia Barbara; C — droga transportowa Gertruda; D — sztolnia Krzyżowa; E — sztolnia Książęca; F — sztolnia Czarna; G — sztolnia Nowa; SMF — sudecki uskok brzeżny

operating from which about 140 kg of gold was obtained annually (L. Bałdys, 1954). Since the beginning of XVIII c., gold production gave place to production of arsenic. As an example, rocks exploited in XVI c. were so highly mineralized with arsenic compounds that approximately contained 40 g/t of Au (L. Bałdys, 1954). In 1514, arsenic ores with 11.4 g/t of Au and in 1744 with 17 g/t of Au were exploited (T. Dziekoński, 1972). During the Inter- the World Wars period, content of gold in 1% arsenic ores was at the level of 0.5 g/t of Au (L. Bałdys, 1954). As economic 7% arsenic ore with content of gold from 3 to 5 g/t was considered (L. Bałdys, 1954). It follows from the known documents that since 1481 to 1944 about 3 800 000 t of arsenic ores and 9–13 t of gold were exploited in the region (L. Bałdys, 1954). After the Second World War economic arsenic ores had an average arsenic content up to 6% and yielded 3.2–3.5 g/t of Au (L. Bałdys, 1954). Gold was chemically identified in loellingite up to 30 g/t of Au and in arsenopyrite from 5.2 up to 34.8 g/t Au (O. Wiencke, 1907; H. Quiring, 1914). H. Budzyńska (1971) as the result of spectrographic investigations determined that main gold concentration occurs in loellingite and glaucopyrite and traces were found in arsenopyrite, glaucodot, pyrite and galenite. On the base of analysis done by I.C.P.-E.A.S., colloidal-size gold in pyrrhotite (up to 52 g/t), pyrite (up to 55 g/t) and in magnetite (26 g/t) was detected (A. Muszer, 1992). Additionally invisible gold (0.4 wt. %) in (Ni, Fe, Co) sulphoarsenides and in bismuthinite (up to 2.3 wt. %) was also described (S. Z. Mikulski, 1995*b*). Investigation made with microprobe observations on samples taken from old waste dumps (A. Muszer, 1992; K. Niczyporuk, S. Speczik, 1993) and from natural outcrops in the near vicinities and from the "Złoty Jar" quarry (S. Z. Mikulski, 1994) proved presence of submicroscopic and microscopic-size particles of native gold. The Złoty Stok As-Au deposit is of the contact metasomatic type and its genesis and metal source are linked with the Kłodzko – Złoty Stok intrusion (A. Neuhaus, 1933; H. Schneiderhöhn, 1955; W. M. Kowalski, 1969; J. Kanasiewicz, 1992; S. Speczik, 1994) or, according to others, ore-formation process begun before intrusion was formed (M. Banaś, 1973; A. Muszer, 1995).

MATERIALS AND METHODS

Over 100 rock samples were collected from the "Złoty Jar" quarry and outcrops nearby in the years 1992–1995. Petrography studies were based on 18 thin sections and over 70 polished sections. The above materials have been partly illustrated on plates. Detailed microscopic studies in reflected light using *LEITZ* microscope of *ORTHOPLAN-PL* type were carried out in order to recognize the composition and succession of ore paragenesis. "Visible" gold was found during studies under the ore microscope in reflected light and than proved by detailed microprobe investigations with use of EDX Link ISIS System coupled with electron microscope of *JEOL JSM-35* in PGI. Additional studies were carried out in Polish Academy of Sciences with use of microprobe An 10/855 Link System connected with *JEOL JSM-840A* under following conditions: accelerating voltage — 20 kV, sample current — 6×10^{-9} and counting time — 20 μs. Study of dispersed gold were carried out with use of equipment and under the same conditions described above.

Preliminary geobarometric measurements on samples supplied by the author were made by A. Kozłowski (1995). Homogenization temperatures were measured with use of micro-

scopic thermocamera made by *Fluid Co.* This allowed for very high accuracy of determined temperature of ±1°C. Th of carbon dioxide inclusions used for *P* determination were made with accuracy of ±0.1°C.

Rock samples for chemical analyses presented in this paper were collected from the I and II exploitation level of the "Złoty Jar" quarry. Especially calc-silicate rocks and rocks containing ore mineralization in form of impregnation and veins were chosen. Chemical gold determination was made in the PGI Central Chemical Laboratory with precision of 1 ppb. Rock samples, after burning at temperatures 450 and 640°C, were digested by HCl concentrate and then dissolved with use of aqua regia. The obtained gold-bearing chloride complex was extracted into organic form. All results were obtained using Flameless Atomic Absorption method (GFAAS) by spectrophotometer *PERKIN ELMER* model *4100 ZL.*

Tungsten was determined with use of Fluorescence Roentgen Spectrophotometer made by *Rigaku Co.* (Japan) under following condition: 200 mA and 50 kV.

GEOLOGICAL SETTING OF THE "ZŁOTY JAR" QUARRY AREA

The "Złoty Jar" quarry of blastomylonitic schist is located in the northern part of the Orłowiec Synclinorium (J. Don, 1964) which is a part of the Złoty Stok – Skrzynka Dislocation Zone (J. Don, 1964; S. Cwojdziński, 1975). Just recently, it was defined as Złoty Stok – Trzebieszowice (ZSTSZ) regional shear zone up to 4 km wide which has NE–SW trend and was developed at the time of the Variscan deformations (Z. Cymerman, 1996). Its northern part is cut by the Sudetic Marginal Fault (SMF) of NW–SE direction (Fig. 1). In the southern part of the ZSTSZ, close to its contact with the Śnieżnik metamorphic complex, occur the Jawornik granitoid (335 Ma; J. Borucki, 1966). From the west, this metamorphic complex is bordered by the Kłodzko – Złoty Stok plutonic massif. These granitoid rocks are cropping out on the surface about 1.5 km to the west from the quarry. The late-tectonic Kłodzko – Złoty Stok massif is an intrusion of mixed granitoids of syntectonic-contamination type (K. Smulikowski, 1979) origin developed along dislocation planes with NW–SE trend, during late phases of the Variscan orogeny (298–262 Ma; T. Depciuch, 1972). Just recently, it was classified as I type granitoid (M. W. Lorenc, 1995). Intruding magma had a high temperature what is marked by reomorphic liquidation of so-called Haniak gneisses, by intensive microclinization, appearance of cordierite, especially in biotite rich rocks, formation of migmatites within biotite schist (M. Kozłowska-Koch, 1973; S. Cwojdziński, 1975; I. Wojciechowska, 1975; B. Wierzchołowski, 1976; K. Smulikowski, 1979), and was responsible for ore forming metasomatic processes on the Złoty Stok As-Au deposit (H. Schneiderhöhn, 1955; W. M. Kowalski, 1963; S. Speczik, 1994).

Excavation works in the "Złoty Jar" quarry begun in 1961 at the same time when decision about closing mining activity in the Złoty Stok As-Au deposit was made. The quarry was open to produce crushed stone from blastomylonitic schist and surrounding rocks for road construction purpose. Actually, in the quarry exploitation is not carrying out. This quarry is over 200 m long and 70 m high and has a moon like shape open to east. Accessible to the observations are three lower levels (380–410 m a.s.l.). Rocks in the quarry belong to the eastern part of the ZSTSZ. The five strongly different rock blocks were

distinguished there (I. Wojciechowska, 1976; J. Żaba, Z. Będkowski, 1995). Each of them is separated by normal faults which are usually dipping (70–80°) to SW. The rock blocks in the central and northeastern part of the quarry are built of blastomylonitic biotite-oligoclase schist, biotite gneiss with number enclosures of amphibolite schist and chlorite-amphibole schist, locally associated with silicate-calcite rocks, amphibolites, and black serpentinites (Fig. 1). In SSW part of the quarry rock blocks are consist mainly of leptynite leuckogneisses with inserts of biotite schist and chlorite-amphibole schist. The rock block located most to SSW is built of biotite-quartz schist and leptynite gneisses. The quarry is located on eastern slopes of the Krzyżowa Mt. between the old Krzyżowa Mt. (Eastern) Ore Field (II) and the Sołtysia Mt. Ore Field (IV) of the "Złoty Stok" mine. In the Eastern Ore Field arsenic ore occurred in several nest-like concentrations. The predominating ores were those occurring in calc-silica rocks, the black and green serpentinites. Contrary to Western Ore Field arsenopyrite and Cu-sulphide dominate here over the loellingite. The ore aggregations have a N–S strike and general dip of 30–40°SW (L. Bałdys, 1954). The arsenic content in ores with disseminated mineralization went up to 7% (L. Bałdys, 1954). The Sołtysia Mt. Ore Field characterized by poorer disseminated sulphide mineralization in diopside-tremolite rocks with arsenic content from 4 to 8%. The ore zone has a NNE–SSW strike and dips towards ENE at the angle of 60–70°E (L. Bałdys, 1954). Influence of the Kłodzko – Złoty Stok granodiorite intrusion in the area of II and IV Ore Fields are much weaker than in the Western Ore Field (W. M. Kowalski, 1961, 1963).

DESCRIPTION AND TEXTURAL STUDY OF GOLD MINERALIZATION

In the "Złoty Jar" quarry ore mineralization was found on the lowest extraction level, within three narrow separate zones, in the band of calc-silicate rocks and pyroxene skarn and in surrounding (S. Z. Mikulski, 1994, in press). Three types of mineralization can be distinguished: disseminated, stringer and on the minor scale massive. Often the two first types occur in the same sample. The former as a wall-rock impregnation and the later as a fracture-fill. These types are superimposed on pre-existing ore mineralization (ilmenite, magnetite, pyrrhotite, pyrite). Epigenetic mineralization of gangue or/and ore veins and veinlets with thickness from a few millimetres up to 2–3 cm in size are hosted mainly by calc-silicate rocks and leptynites. Mineralization textures indicate a succession of cycles of ductile-brittle and brittle deformation and hydrothermal infill. Most interesting are rocks appearing in the central part of the quarry. These rocks are represented by diopside skarn and diopside ± tremolite ± calcite ± talc rocks of light green colour. They occur in form of lens about 1 m thick and are enveloped by amphibole-chlorite schist and leptynite gneiss (85°/60–65°SW). Within these rocks nest-like zone of intensive silicification and carbonatization about 1.5 m thick was observed. Locally, the massive ore mineralization also occur within zone up to a few tens of centimetres, as dense disseminated impregnation, thick spots, and nests as well. The main ore minerals are: arsenopyrite, loellingite and pyrite. Less frequently occur scheelite and sulphoarsenides, pyrrhotite, chalcopyrite, sphalerite, and magnetite. In black-serpentinite rocks predominate magnetite mineralization.

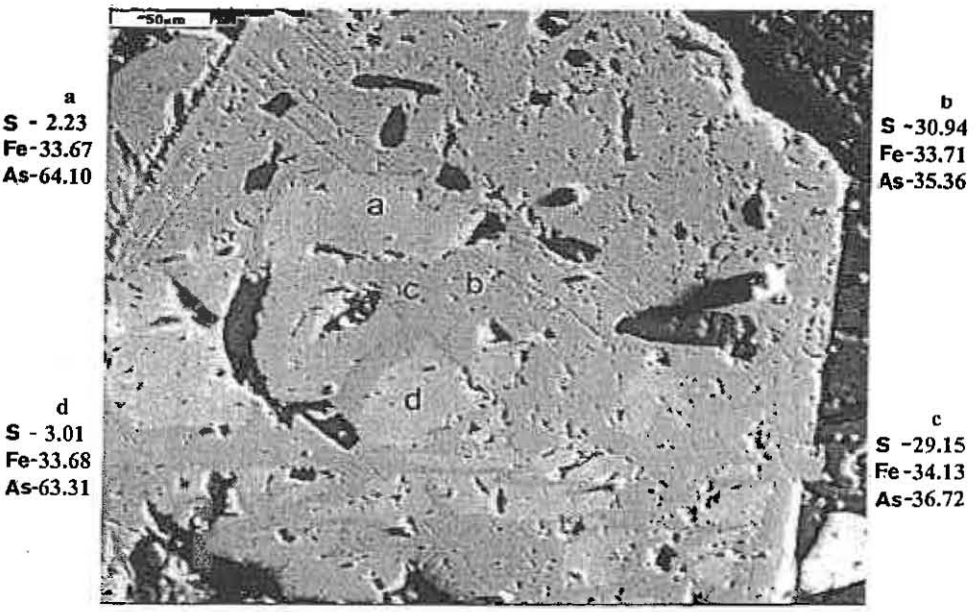

Fig. 2. Replacement of loellingite (light grey) by arsenopyrite (dark grey) with content of elements in indicated points (S, Fe, As in at. %); microprobe analysis (BEI)

Zastępowanie löllingitu (jasnoszary) arsenopirytem (ciemnoszary) z zaznaczoną zawartością pierwiastków (S, Fe, As w % atom.) na podstawie wyników badań w mikroobszarze (obraz BEI)

Arsenopyrite is the principal component of the ore and shows the most characteristic textures. Textural relationships between arsenopyrite and gangue or host correspond to the types: disseminated, stringer or fine-banded and massive ores. Disseminated type (a) is characterized by finely disseminated arsenopyrite grains usually idiomorphic from a few micrometres up to millimetres in size and aggregates (up to 5.X cm) which may form lenticular shapes (Pl. II, Fig. 14a). Bigger arsenopyrite grains are usually crushed down to microclasts. Often related to hydrothermal infilling structures which are usually not parallel to rock texture. In the "Złoty Jar" quarry it is a big importance. Different forms have irregular arsenopyrite concentration within loellingite and its marginal parts (Pl. I, Fig. 13a–d). Loellingite-arsenopyrite coarse-grain aggregates occur commonly in calc-silicate rocks and their relation is changeable. In the central part of some younger arsenopyrite grains the remnants of loellingite were observed (Fig. 2). SEM studies of arsenopyrites, disseminated in calc-silicate rocks, allow to detect among them compositional differences (Fig. 3a). Chemical composition of arsenopyrite crystals is shown on the ternary Fe-As-S phase diagram on Figure 3b. Content of arsenic is 46.40–51.62 wt. %, sulphur 15.89–18.64 wt. % and iron 32.59–34.64 wt. %. Traces of Au, Sb (up to 0.19 wt. %), Co and Ni were detected (Fig. 3c). Chemical formula of arsenopyrite (I): $Fe_{0.99-1.4}As_{1.05-1.10}S_{0.88-0.96}$.

Single idiomorphic crystals of the younger arsenopyrite generation also occur as impregnation in calc-silicate rocks but exhibit lower arsenic content and enrichment in

a

at. %			wt. %			
S	Fe+Co+Ni	As	S	Fe+Co+Ni	As	Total
30.94	33.71	35.36	17.80	33.79	47.54	99.13
29.15	34.13	36.72	16.68	34.02	49.11	99.81
30.45	33.61	35.94	17.43	33.51	48.07	99.01
31.93	34.06	34.01	18.84	34.64	46.40	99.88
29.68	34.02	36.30	17.22	34.39	49.22	100.83
30.82	33.69	35.49	17.97	34.21	48.34	100.52
29.75	33.99	36.27	16.99	33.80	48.39	99.18
30.62	34.02	35.36	17.73	34.30	47.84	99.87
32.03	32.94	35.04	18.33	32.84	46.86	98.03
31.06	33.63	35.12	17.81	33.60	47.07	98.48
31.11	33.73	35.15	17.82	33.66	47.05	98.53
33.63	33.80	32.57	19.37	33.90	43.83	97.10
34.60	33.60	31.80	19.99	33.80	42.92	96.71
34.45	33.25	32.30	20.18	33.93	44.20	98.31
34.24	33.61	32.14	20.17	34.48	44.24	98.89

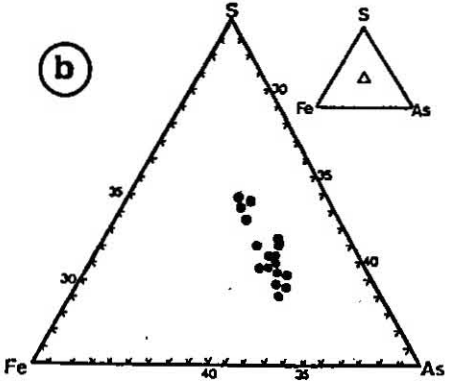

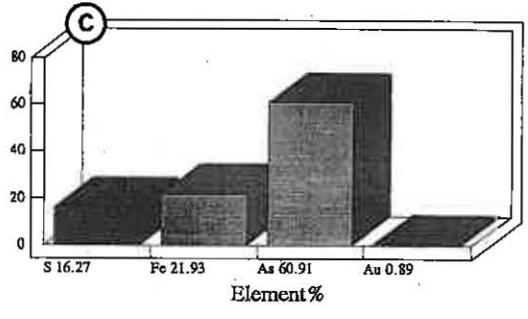

Fig. 3a–c. Arsenopyrite composition: a — electron microprobe analyses of arsenopyrite; b — Fe-As-S graph of individual microprobe analyses (at. %); c — quantitative microanalysis of arsenopyrite with increased content of Au (EDS)
Skład chemiczny arsenopirytu: a — tabela wyników badań w mikroobszarze; b — skład arsenopirytu w % atom. w trójkącie Fe-As-S; c — wyniki mikroanalizy ilościowej arsenopirytu z podwyższoną zawartością Au (EDS)

sulphur. The content of As is from 42.92 up to 44.4 wt. %, S — 19.37–20.18 wt. %, and Fe — 33.80–34.48 wt. %. Chemical formula of arsenopyrite younger generation: $Fe_{1.00-1.01}As_{0.95-0.98}S_{1.01-1.04}$.

The following younger generation of arsenopyrite revealed textures which contribute to a typological classification scheme of shear-zone gold ores (R. Castroviejo, 1990). The stringer or fine-banded type (b): arsenopyrite or scheelite (II) grains occur as an infill in microfissures and veinlets with widths from micrometres up to 3 mm (Fig. 4c; Pl. II, Fig. 14b, c). It was also found arsenopyrite intergrowths with loellingite as fillings of fissures and voids in cracked earlier crystallized grains of $FeAs_2$. Within this generation of arsenopyrite, "visible" native gold inclusions were sporadically observed. Massive ores type (c): arsenopyrite occur in thick spots or nests of millimetres/centimetres thickness. These forms are built of coarse-grained aggregates, intergrowths with other ores and with gangue (Pl. II, Fig. 14d).

Loellingite is subordinate with respect to arsenopyrite although being in places the principal component. Loellingite occurs in grains of columnar and acicular habits, which are loose disseminated in rocks in the form of impregnation or nest-like concentration of radial-concentric shaped (up to several centimetres in size) (Pl. II, Fig. 14a–d). Columnar crystals of loellingite rich up to 3 cm of length and up to 0.5 cm of thickness. Lower sizes (0.0X–2.X mm) have loellingite grains of needle shape. Coarse grains are cataclased and cemented by a younger generation of gangue (quartz, calcite) or arsenopyrite. Under the ore microscope some of loellingite crystals revealed heterogeneous composition what is shown by different optical features. Microprobe analyse proved these observations. Darker irregular parts of loellingite grain are richer in sulphur and relatively poorer in arsenic content (iron content is at the same level). These concentrations are formed by arsenopyrite. Determination of chemical composition of loellingite revealed arsenic, iron and sulphur contents around 70.48–72.96, 27.68–28.21, and 1.07–1.45 wt. %, respectively (Fig. 2b, d). Formula of loellingite: $Fe_{0.99-1.0}(As_{1.9-1.93}S_{0.07-0.09})_{1.99-2.01}$.

Scheelite is the next ore mineral and for the first time was described from the Złoty Stok deposit area by S. Z. Mikulski (1994). Scheelite occurs most commonly in forms of individual impregnation, thick spots and nest-like crystalline grains and veinlets (Fig. 4c). Two generations of scheelite were observed. The first one appears as less or more idiomorphic single grains from 0.0X up to a few millimetres in size. Bigger ones are solid crystalline aggregates up to 2–3 cm. Scheelite intergrowths with pyrite were sporadically observed, despite its common intercalations with quartz or calcite. These mineral aggregates are often tectonically fractured, exhibit signs of fissure fills by younger generation of calcite (Pl. III, Fig. 15a). Scheelite II generation appears close in association with quartz or quartz and calcite in form of incrustation in central part of epigenetic veinlets and as irregular fillings of voids in calc-silicate rocks (Fig. 6b; Pl. III, Fig. 15b). These veinlets are usually from 0.X up to 2.X mm thick. The results of microprobe analysis of scheelite I revealed its inhomogeneous chemical structure with admixture of Mo up to 4.5 wt. % and traces of Cu, Sr, Y (S. Z. Mikulski, 1995*a*) (Fig. 4a, b). Scheelite I crystals contain WO_3 from 80.97 up to 83.08 wt. % and CaO from 17.30 up to 18.91 wt. %.

(Ni, Fe, Co) sulphoarsenides appear in the light green calc-silicate rocks in the form of filling of microfissures in association with pyrite, calcite and as single or thin aggregate concentration (Pl. IV, Fig. 16c). Sulphoarsenide grains have sizes from 0.0X up to 2.X mm,

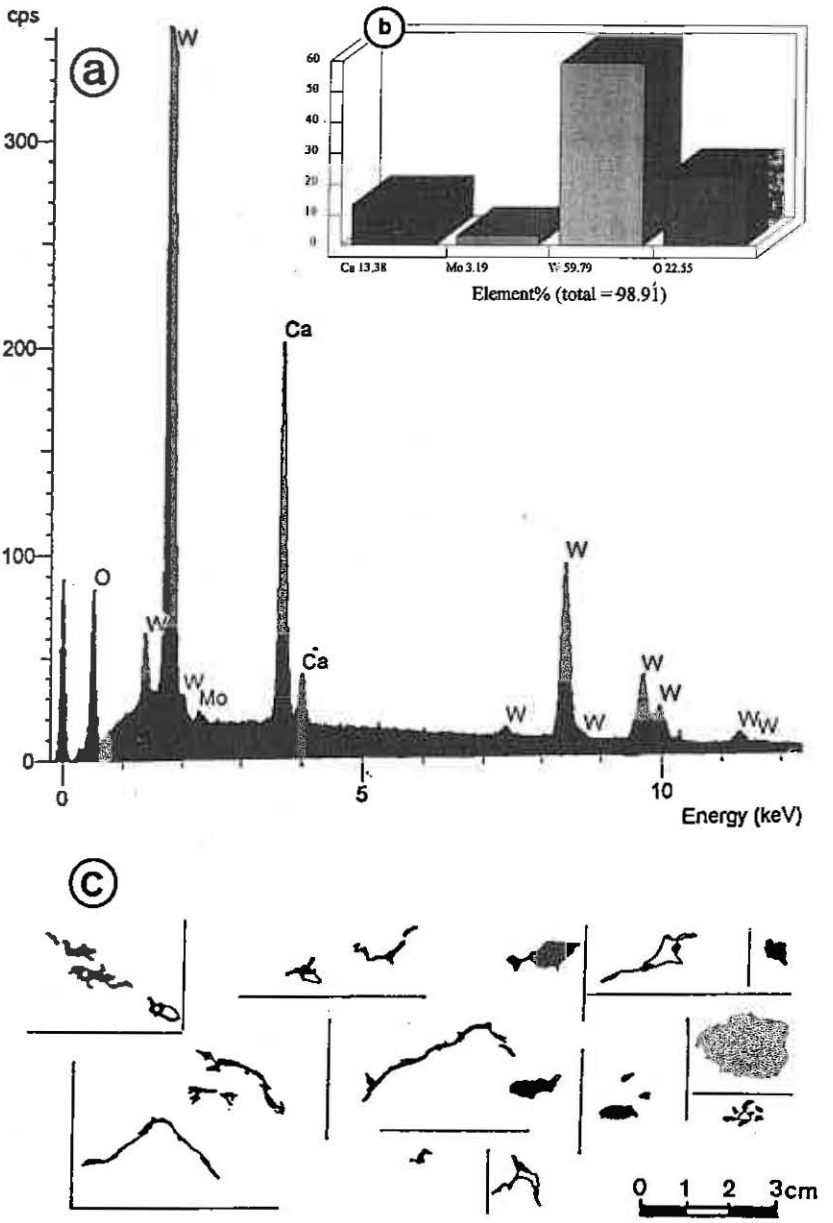

Fig. 4a–c. Scheelite from the "Złoty Jar "quarry: a — composition of scheelite as revealed by microprobe studies (EDS spectrum); b — quantitative microanalysis of scheelite with increased content of Mo (EDS); c — scheelite occurrences in the forms of spot, nest or veinlet which infill voids and microfissures in calc-silicate rocks

Scheelit z kamieniołomu „Złoty Jar": a — skład scheelitu na podstawie badań w mikroobszarze (widmo EDS); b — wyniki mikroanalizy ilościowej scheelitu z podwyższoną zawartością Mo (EDS); c — plamiste, gniazdowe i żyłkowe formy wystąpień scheelitu wypełniające mikrospękania i pustki międzyziarnowe w skałach węglanowo-krzemianowych

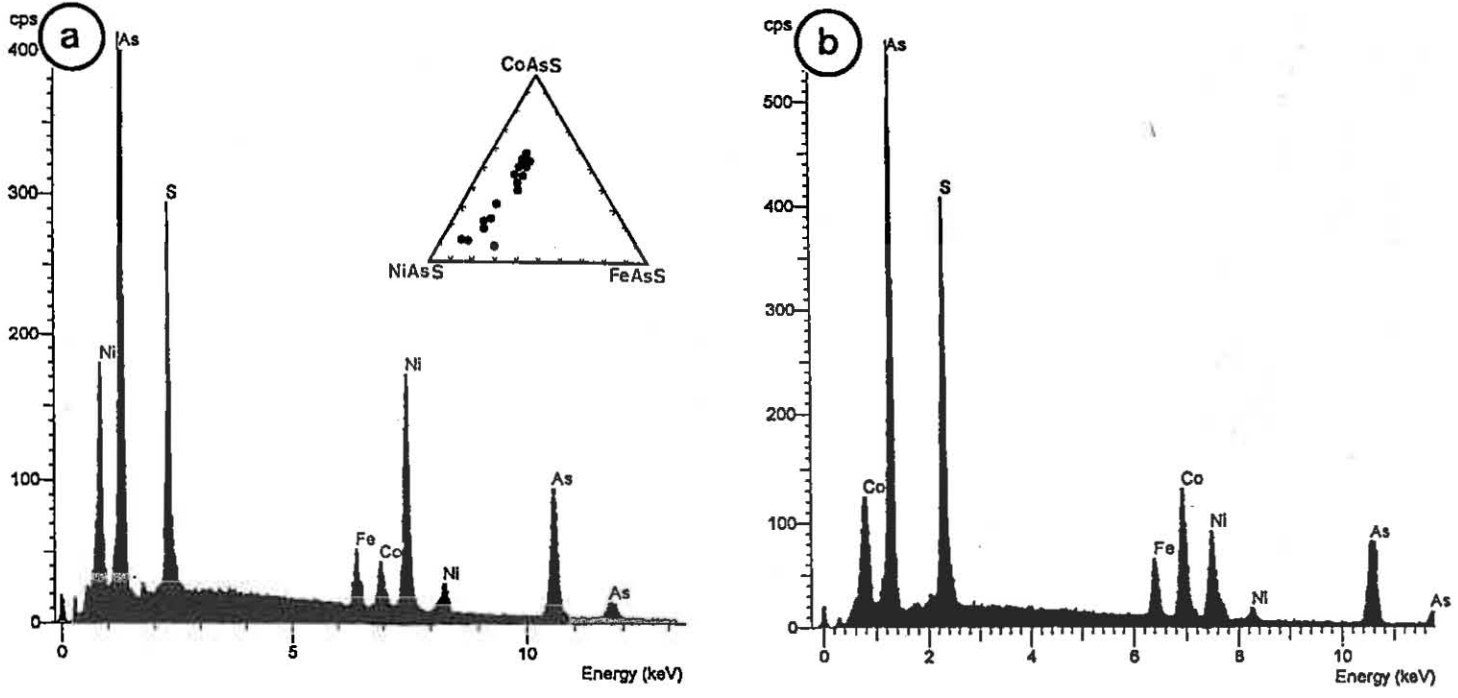

Fig. 5a, b. Composition: a — of Co-gersdorffite as revealed by microprobe studies; in upper corner — NiAsS-FeAsS-CoAsS diagram with projection points of Co-gersdorffite and Ni-cobaltite; b — of Ni-cobaltite as revealed by microprobe studies

Skład: a — Co-gersdorffitu na podstawie badań w mikroobszarze; w górnym rogu — diagram trójkątny w układzie NiAsS-FeAsS-CoAsS z zaznaczonymi punktami Co-gersdorffitu i Ni-kobaltynu; b — Ni-kobaltynu na podstawie badań mikrosondą

and usually normal habit with inhomogeneous chemical structure (Fig. 5a, b; Pl. IV, Fig. 16a, b). Under the ore microscope each of this zone shows a slightly different reflectivity, colour, isotropy or weak anisotropy. The most characteristic optical feature in the reflected light is their white colour with rose or rose-creamy tint intensified in immersion. Sulphoarsenides are represented mainly by a series of different Ni, Co and Fe compounds. These minerals may be placed among the minerals of the **cobaltite-gersdorffite** series (D. Klemm, 1965). Most often **Ni-cobaltite** and **Co-gersdorffite** were observed. Internal part of such sulphoarsenide grains is built by **Co-gersdorffite** with higher content of As (51–63 wt. %), Ni (19–28 wt. %) and lower of Co (3–8 wt. %) and Fe (2–8 wt. %) (Pl. IV, Fig. 16a, b). Chemical formula of Co-gersdorffite: $(Ni_{0.66-0.85}Fe_{0.08-0.26}Co_{0.09-0.23})_{0.86-1.1}(As_{1.18-1.61}Bi_{0.00-0.01})_{1.18-1.62}S_{0.52-0.79}$.

Such core is covered by **Ni-cobaltite** rim with content of As 47–49 wt. %, Co 17–21 wt. %, Ni 9–14 wt. %, Fe 5–6 wt. %, and S 15–16 wt. % (Pl. IV, Fig. 16a, b). Chemical formula of Ni-cobaltite: $(Ni_{0.28-0.40}Fe_{0.17-0.19}Co_{0.5-0.6})_{1.04-1.08}As_{1.08-1.11}S_{0.81-0.86}$.

Outer part is characterized by an increase in Co and decrease of Ni component. Au, Ag, Bi, Cu, and W admixtures were also determined (S. Z. Mikulski, 1995*b*). Some of analyzed grains have more homogeneous structure and content of Ni 11.95–14.85 wt. %, Co 14.04–16.47 wt. %, Fe 6.7–7.2 wt. %, As 47.8–50.1 wt. %, S about 15 wt. %. Chemical formula of this mineral: $(Ni_{0.35-0.44}Fe_{0.21-0.22}Co_{0.41-0.49})_{1.05-1.07}As_{1.1-1.11}S_{0.81-0.85}$.

Microscopic observation proved by chemical analysis allowed to notice that chemical hydrothermal remobilization of Ni, Co, Fe, As, and S from primary ore minerals are responsible for crystallization of these minerals in lower temperatures.

Bismuthinite and native bismuth formed fine irregular, denticulate or spongy shaped inclusion in (Ni, Fe, Co) sulphoarsenides.

Pyrite commonly was found in association with arsenic and sulphoarsenide minerals. Beside, its idiomorphic grains up to a few millimetres in size occurs also as solid coarse-aggregates up to 5 cm big and in form of veinlets as well. Pyrites of different generation appear in intergrowths with arsenopyrite, chalcopyrite or pyrrhotite.

Chalcopyrite, pyrrhotite, sphalerite and **magnetite** occur less frequently and as disseminated impregnation in form of individual grains or intergrowths (up to 1.X mm in size) in calc-silicate and skarn rocks. Some of these minerals appear in a few generations (Fig. 7).

Titanite occurs in silicificated and carbonated zones in form of single idiomorphic crystals up to 1.X mm in size with very characteristic rhombic sections.

"VISIBLE" GOLD

Native gold grains and inclusions were observed as infill of microfractures, within disseminated or veinlet ore mineralization in pyroxene-garnet skarn and diopside ± tremolite ± calcite ± talc rocks from the central part of the quarry lowest exploration level. Most often, Au inclusions appear in aggregates of (Ni, Fe, Co) sulphoarsenides between zones of Co-gersdorffite and Ni-cobaltite (Pl. V, Fig. 17a–c). Individual gold grains are larger and were noticed in epigenetic quartz ± calcite veins (Fig. 6a; Pl. V, Fig. 17d). Under the ore microscope the colour of native gold polished surface is a luminous golden yellow much

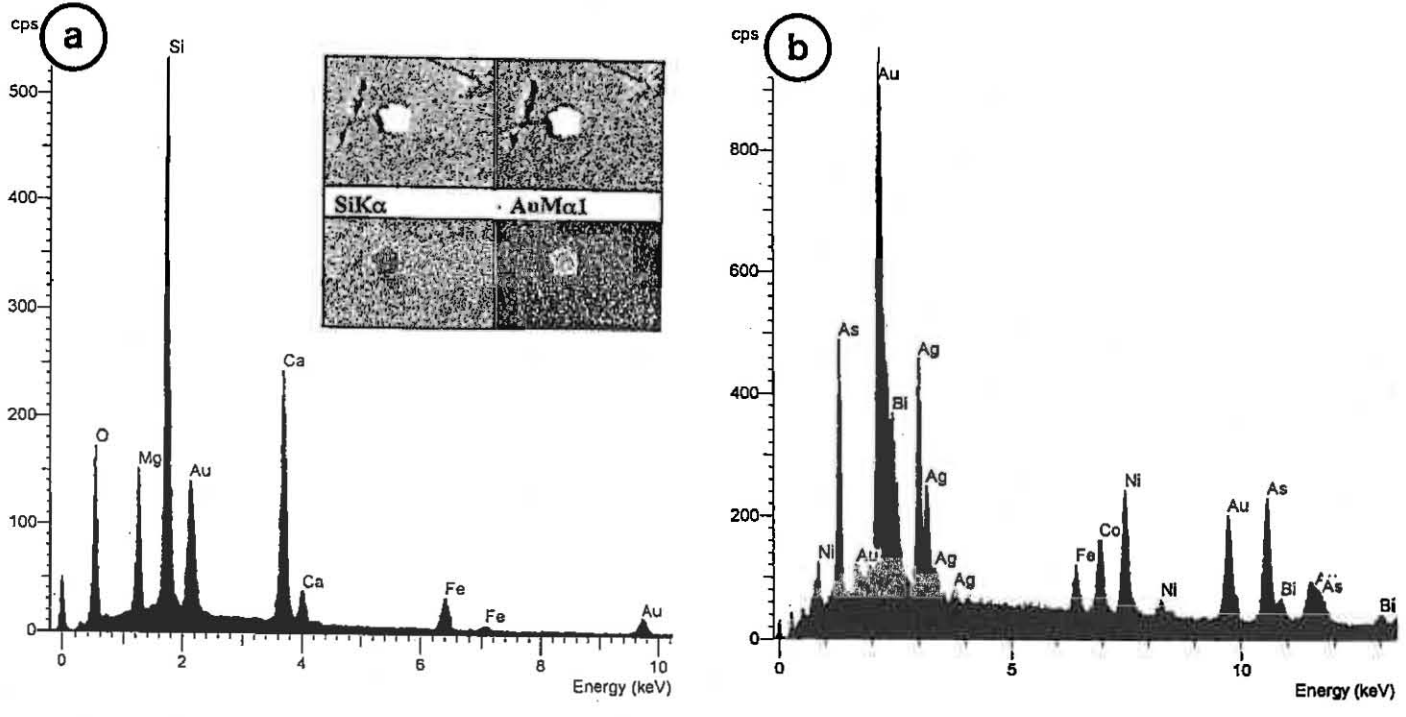

Fig. 6a, b. EDS spectrum: a — of native gold in diopside; in upper corner — distribution maps of characteristic SiKα and AuMα1 radiation; x 1600; b — of electrum in Ni-Fe-Co sulphoarsenides

Widmo EDS: a — złota rodzimego w diopsydzie; w górnym rogu — mapy rozkładu promieniowania charakterystycznego SiKα i AuMα1; 1600 x; b — elektrum w siarkoarsenkach Ni-Fe-Co

variable with the silver content, the reflectivity is enormously high (P. Ramdohr, 1969). Usually, two or more native gold inclusions were observed in individual grains of (Ni, Fe, Co) sulphoarsenides. Some of them have a strong white tint what indicate higher silver admixture and was proved by microprobe analyse (up to 31.6 wt. % of Ag and from 3.8 up to 4.5 wt. % of Bi) (Fig. 6b). It is worthy to notice the constant admixtures of As up to 1.93 wt. %, Ni — 1.57 wt. %, and W — 1.34 wt. %. According to P. Ramdohr (1969) such high Ag-content in native gold indicates presence of electrum (30–45 wt. % of Ag). Electrum inclusions have from 0.5 up to 20 μm in sizes and curvilinear elongated forms (Pl. IV, Fig. 16c). Beside, inclusions of native gold with admixture of Ag and Bi also gold-bismuth myrmekites within sulphoarsenides were observed. These intergrowths reach up to 5 μm in size. In natural occurrences such structures form as a result of solid solution decomposition of maldonite (Au_2Bi) (P. Ramdohr, 1969). Usually it is found that maldonite is decomposed into a predominantly coarse myrmekite of Au and Bi with ~1:1 surface proportion. Smaller and larger intact remnants occur only in wedges. The formation of maldonite is apparently limited to a narrow margin within the high temperature range (P. Ramdohr, 1969). In the pole part content of bismuth in native gold reaches up to 30.5 wt. % or up to 33.8 wt. % of gold admixture in bismuth. Non numerous grains of native gold observed in quartz ± calcite veinlets were bigger (5–50 μm in size) and characterized by more intensive yellow colour, lower admixture of other elements up to 15 wt. %. Native gold grains have most often oval shape with more or less regular edges (Pl. V, Fig. 17d). One gold grain found in diopside has much lower size — 2 μm in regard to this tests of microprobe analysis came to grief (Au < 60 wt. %) (Fig. 6a). The visible gold contained within loellingite is interpreted to have been released during replacement by arsenopyrite. During progressive sulphidation of the loellingite the arsenopyrite grain boundary against the loellingite migrated towards the core of the loellingite.

SEQUENCE OF CRYSTALLIZATION

Paragenetic sequence of the main minerals in calc-silicate and skarn rocks from the "Złoty Jar" quarry is shown in Figure 7. The sequence of crystallization of the gold-bearing minerals described above may be divide into three main stages. Stage I was developed in result of different metasomatic type of the fluid fronts (at about 500°C and low salinity, see below) connected with granodiorite intrusion which replace primary calcareous rocks into calc-silicate and pyroxene-garnet skarn rocks. This stage may be divide into:

a — calc-silicate sub-stage A (pyroxene — diopside, garnet, quartz, and calcite);

b — oxide sub-stage B (magnetite, "invisible" gold(?), scheelite, titanite, powellite, quartz, and calcite);

c — sulphide sub-stage C (pyrrhotite, loellingite, arsenopyrite, glaukodote(?), gersdorffite, "invisible" gold, pyrite, chalcopyrite, sphalerite, native gold, and quartz).

A core of corroded loellingite can be found in calc-silicate rocks, indicating that the reaction loellingite plus pyrrhotite to form arsenopyrite took place. The minerals of Fe-As-S system are followed by chalcopyrite, pyrite. The regional metamorphism and the subsequent dynamic metamorphism (strong mylonitization) related to the emplacement of granodiorite intrusion and development of the ZSTSZ in the Variscan time constitute a frame of reference

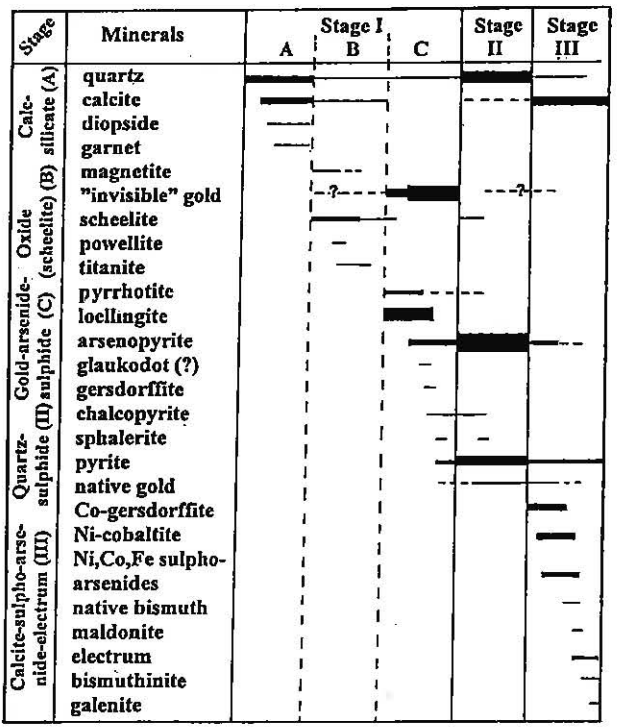

Fig. 7. Paragenetic sequence of the main minerals in the gold-bearing calc-silicate rocks from the "Złoty Jar" quarry
Schemat sukcesji złotonośnej mineralizacji w skałach węglanowo-krzemianowych z kamieniołomu „Złoty Jar"

for the late-stage cataclasis ores (II, III), according to the brittle deformational effects produced in them. Stage II is represented by quartz, quartz-calcite or green serpentine veinlets also containing ore minerals such as: arsenopyrite, pyrite, native gold, chalkopyrite or scheelite and on the minor scale pyrrhotite and sphalerite. There is no big difference between the ore minerals content of different zones. Stage III was marked by an increase in the content of barren calcite or calcite enriched in Ni-Fe-Co sulphoarsenides and inclusions of native gold. Among ore minerals the main role are played by pyrite, Co-gersdorffite, Ni-cobaltite, native gold, native bismuth, electrum, maldonite, bismuthinite, and galenite. The overall ore-mineralization of stage I, II and III permits to include such mineralization to tectonic and hydrothermal evolution within transition from ductile-brittle to brittle condition by hydrothermal circulation and accumulation of ores.

ARSENOPYRITE GEOTHERMOMETER

The As/S ratio of the arsenopyrite coexisting with other phases in the system Fe-As-S has been experimentally calibrated as a geothermometer by U. Kretschmar and S. D. Scott (1976). However, application is often rather problematic. Among the main problems is the widespread presence of significant amounts of other elements within arsenopyrite. Furthermore, arsenopyrite is very often zoned with respect to As content and true buffered assemblages are often hard to find. Within the studied samples, only a few arsenopyrite grains disseminated in calc-silicate rocks seems to be suitable for geothermometry; the majority being excluded because of high Co contents or unclear paragenetic relationships with neighbouring minerals. Arsenopyrites from veinlets were not investigated here. Conditions close to loellingite + pyrrhotite + arsenopyrite (lö + po + asp) equilibrium have been assumed for the arsenopyrite which also contains relicts of loellingite. Arsenopyrite I shows compositional variation with a mean of 35.53 at. % As ($2\sigma = \pm 1.52$) (Fig. 3a). According to the scheme (Fig. 8a) arsenopyrite I could have originated at temperatures of about 420 to 530°C and was calculated using lö + po + asp buffering curve. However, the $\log fS_2$ values indicated their crystallization in lower temperatures ranging from 400–440°C. U. Kretschmar and S. D. Scott (1976) notes that such arsenopyrite contain more As than arsenopyrite formed together with pyrite. This conclusion is supported by the data in Figure 3a. Arsenopyrite II ($\bar{x} = 32.20$ at. % As; $2\sigma = \pm 0.64$) temperatures calculated using the po + asp + py buffering curve are lower compared to arsenopyrite I (from 415 up to 455°C). As arsenopyrite was considered pure $FeAsS_2$ in the experimental calibration, it is not possible to confirm the S content of this mineral, that this assemblage was actually in equilibrium. The temperatures received on diagram of isopleths of atomic As in arsenopyrite in a sulphur fugacity versus temperature (U. Kretschmar, S. D. Scott, 1976) are outside the stability field of arsenopyrite (315–325°C). In the Figure 8b arsenopyrite compositions in atomic percentage in the ternary system Fe-As-S from the "Złoty Jar" quarry are presented to compare with other deposits according to Z. D. Sharp *et al.* (1985). Two groups of arsenopyrites with different contents of As and S from the "Złoty Jar" quarry are visible.

PRELIMINARY RESULTS OF GEOBAROMETRIC STUDIES

The majority of the fluid inclusion studies have been made on quartz from veinlets but scheelite, pyroxene, and garnet from calc-silicate rocks were also included, although lack of clarity of these minerals made measurement of homogenization and particularly melting temperatures difficult. Micrometry data reported here refers only to inclusions classified as primary (syngenetic with its host-mineral — A. Kozłowski, 1995). Th data are shown for quartz, pyroxene, scheelite and garnet in Figure 9a. Fluid inclusions in quartz from veinlet have a Th value from 330–296°C, corresponding to a salinity 4.8–8.6 wt. % NaCl equiv. The limited Th data obtained for garnet show range of 352–316°C (2.4–5.7 wt. % NaCl equiv.). Fluid inclusions in scheelite have Th from 346–328°C (5–5.4 wt. % NaCl equiv.). Th measurements for pyroxene have a range 365–329°C (4.9–6.3 wt. % NaCl equiv.). Lower temperatures have fluid inclusions in quartz containing arsenopyrite mineralization from

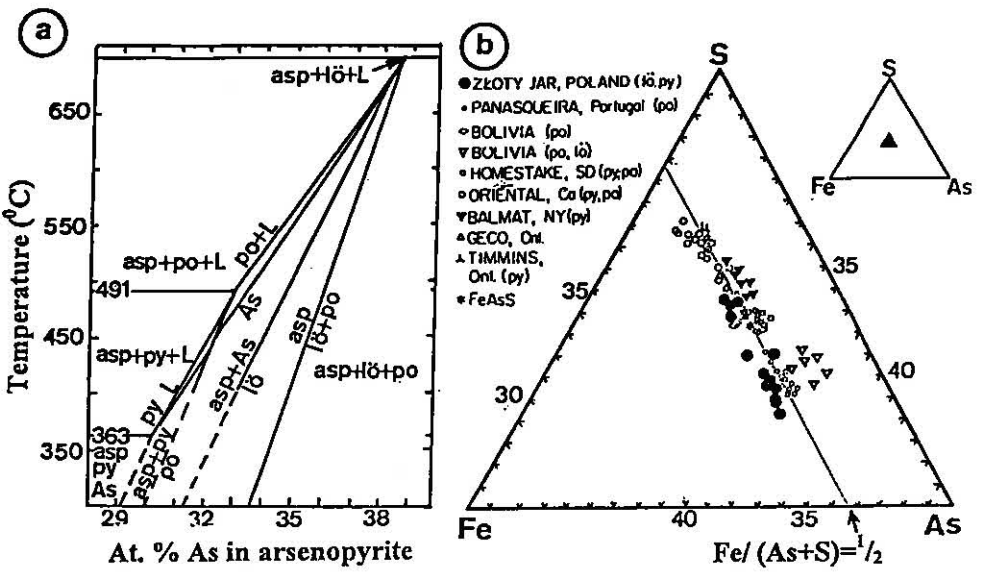

Fig. 8a, b. Arsenopyrite geothermometer: a — phase diagram of dependence of As (at. %) in arsenopyrite composition on temperature (°C) (U. Kretschmar, S. D. Scott, 1976); b — arsenopyrite compositions (at. %) in the ternary system Fe-As-S; coexisting phases shown in parentheses (according to Z. D. Sharp *et al.*, 1985); arsenopyrites from the "Złoty Jar" marked by the author

po — pyrrhotite, lö — loellingite, L — sulphur-arsenic liquid, py — pyrite, asp — arsenopyrite, As — at. % As in arsenopyrite

Geotermometr arsenopirytowy: a — diagram fazowy zależności zawartości arsenu w arsenopirycie (% atom.) od temperatury (°C) (U. Kretschmar, S. D. Scott, 1976); b — skład arsenopirytu (% atom.) w systemie Fe-As-S; współwystępujące fazy podano w nawiasach (według Z. D. Sharpa i in., 1985); arsenopiryty ze „Złotego Jaru" zaznaczone przez autora

po — pirotyn, lö — löllingit, L — roztwór siarka-arsen, py — piryt, asp — arsenopiryt, As — % atom. As w arsenopirycie

veinlets representing younger generation. Th temperatures ranges from 288–254°C (3.8–6.6 wt. % NaCl equiv.). To the same range Th temperatures but of higher salinity (7.0–9.5 wt. % NaCl equiv.) corresponds fluid inclusions in quartz containing arsenopyrite mineralization from the Western Ore Field. Lowest Th temperatures show quartz from younger generation of veinlets 234–206°C (3.1–5.6 wt. % NaCl equiv.).

Fluid inclusions data in pyroxene, scheelite and garnet are hosted by quartz-silicate and skarn rocks indicating deposition at Th temperatures of about 364–316°C from fluids contain 2.4–8.1 wt. % NaCl equiv. The Th-salinity diagrams for the skarn mineral assemblages (pyroxene, scheelite, garnet) show increasing salt concentrations in the aqueous phase of inclusions with decreasing temperatures. Using the method of intersecting isochores of aqueous and carbonic fluid inclusions temperatures of pyroxene, scheelite, garnet, quartz and pressures of their crystallization have been established (Fig. 9b). Scheelite is the principal tungsten mineral and fluid inclusion data indicating deposition at temperatures of about 473°C from a fluid contain about 5.2 wt. % NaCl equiv. in pressure of 1.24 kbar.

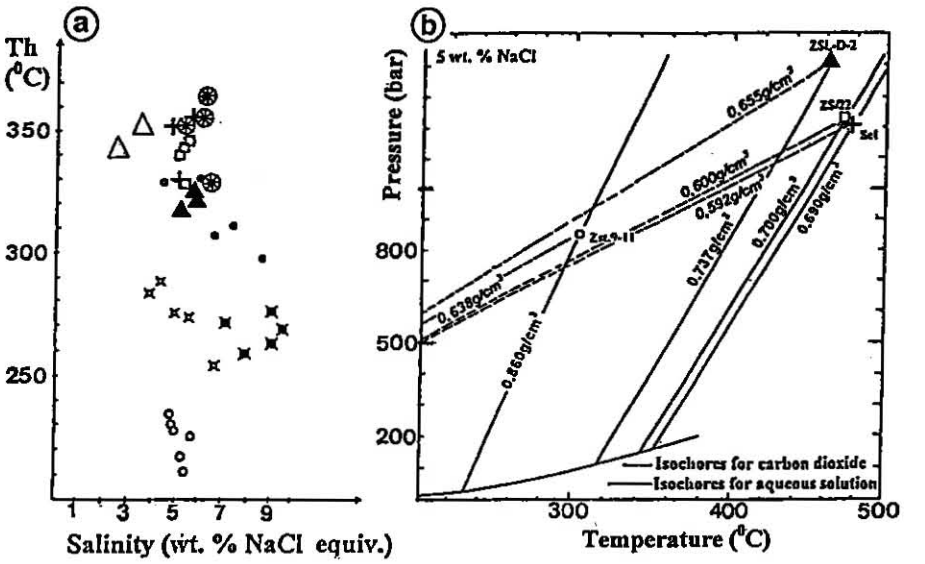

Fig. 9a, b. Fluid inclusion results: a — microthermometry data for pyroxene (wheels, crosses), garnet (triangles), scheelite (squares) and quartz (circles, asterisks) stages; homogenization temperature versus salinity plot; b — estimation of pressure and temperature using the method of intersecting isochores (symbol explanations the same as for a)

ZS/22, ZSL-D-2, Zst9-11, and Sel — samples number's

Wyniki badań inkluzji fluidalnych: a — dane mikrotermiczne dla piroksenu (kółka kierownicy, krzyżyki), granatu (trójkąty), scheelitu (kwadraty) i kwarcu (kółka, gwiazdki); wykres temperatur homogenizacji inkluzji i ich zasolenia; b — określenie ciśnień i temperatur krystalizacji minerałów na podstawie przecięcia odpowiednich isochor (objaśnienia symboli jak przy a)

ZS/22, ZSL-D-2, Zst9-11 i Sel — numery próbek

Pyroxene was formed during the similar conditions at 480°C and 1.22 kbar from fluid containing 4.9 wt. % NaCl equiv. Garnet was formed in a lower temperature at 464°C and pressure of 1.32 kbar from fluid containing 5 wt. % NaCl equiv.

These values of temperatures are close to crystallization conditions of loellingite + pyrrhotite + arsenopyrite (I) association.

"INVISIBLE" GOLD IN ORE MINERALS

The term "invisible" gold is applied to that which occurs either as submicroscopic inclusions within the host mineral or as a solid solution or chemically bound gold, thus rendering the gold refractory to conventional cyanidation (Z. Johan *et al.*, 1989). "Invisible" gold was found in loellingite, arsenopyrite, bismuthinite, and (Ni, Fe, Co) sulphoarsenides in calc-silicate and skarn rocks from the quarry. Highest gold content was determined in bismuthinite and arsenopyrite (Fig. 10a). But some results of the gold determination had a very low precision even ±0.84 wt. %. Bismuthinite grains contained from 0.94 up to 2.22

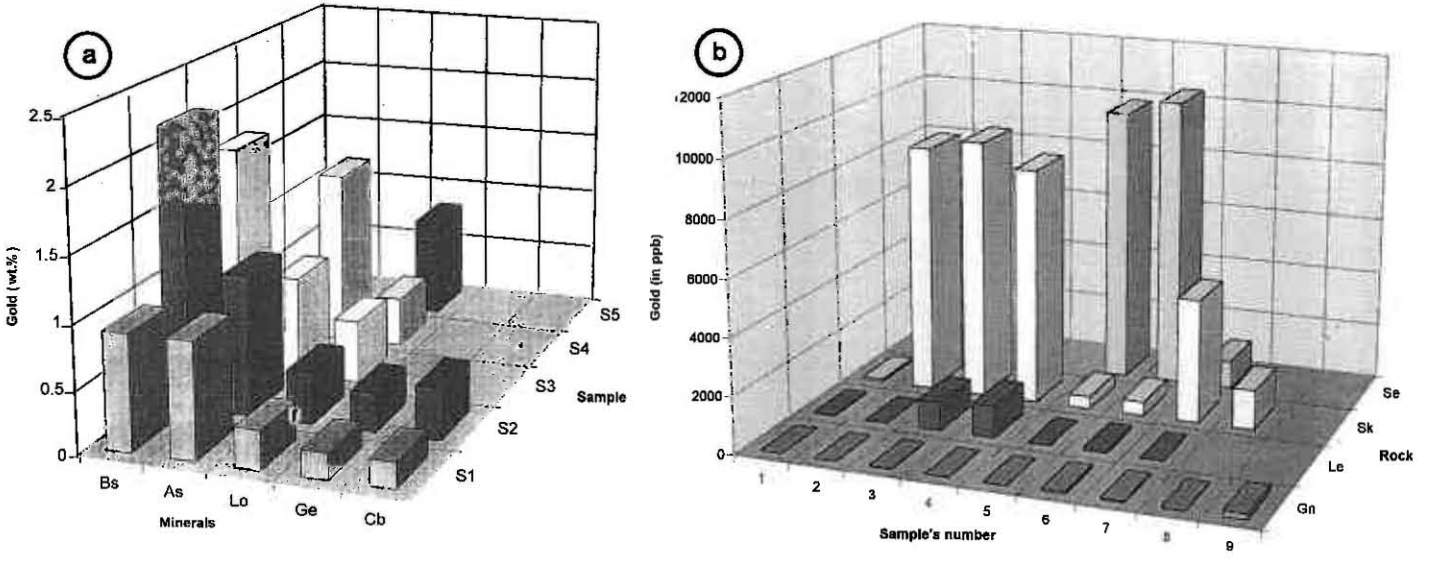

Fig. 10a, b. Histographs of the "invisible" gold concentration in the "Złoty Jar" quarry: a — gold content in ore minerals (wt. %); b — gold content in rocks (ppb)
Bs — bismuthinite, As — arsenopyrite, Lo — loellingite, Ge — Co-gersdorffite, Cb — Ni-cobaltite, Gn — gneisses, Le — leptynites, Sk — calc-silicate rocks, Se — black serpentinites

Histogramy koncentracji złota „niewidzialnego" w kamieniołomie „Złoty Jar": a — zawartość złota w minerałach kruszcowych (% wag.); b — zawartość złota w skałach (ppb)
Bs — bismutynit, As — arsenopiryt, Lo — löllingit, Ge — Co-gersdorffit, Cb — Ni-kobaltyn, Gn — gnejsy, Le — leptynity, Sk — skały węglanowo-krzemianowe, Se — czarne serpentynity

wt. % of Au ($x_{n=3}$ = 1.65 wt. %) and high admixture of Ag up to 2.93 wt. %. Gold content in arsenopyrites from the "Złoty Jar" quarry was from 0.82 up to 1.4 wt. % ($x_{n=5}$ = 0.83 wt. %). Detectable amounts of gold were found mainly in the fine-grained arsenopyrites of prismatic habits. Coarse-grained aggregates of arsenopyrite rarely contained measurable gold. First generation of arsenopyrite contain more chemically bound gold than the second one. Probably, it was due to higher arsenic content 46.40–51.62 wt. % in arsenopyrite (I). By comparison arsenopyrite II contains from 42.92–44.24 wt. % of As. In grains of arsenopyrite (I) Co and Sb admixtures were also determined. The relation was noticed that zone of crystals with the relative highest content admixtures usually has the lowest content of Au. Point analyses of a few loellingite grains confirmed also Au admixture up to 0.72 wt. % ($x_{n=12}$ = 0.224 wt. %). Traces of chemically bound gold in (Ni, Fe, Co) sulphoarsenides were also determined (0.16–0.4 wt. %). A visual examination allows to consider gold-bearing arsenides and sulphoarsenides mineralization, as contact metasomatic and hydrothermal types and include into a group of syn- and post-mylonite related to the late cataclasis.

CHEMICAL DETERMINATION OF GOLD IN ROCK SAMPLES

Highest gold concentrations in calc-silicate and skarn from the "Złoty Jar" quarry rocks were determined in samples contained massive ore mineralization (loellingite-arsenopyrite aggregates). In three samples shown on Figure 10b the gold concentration was more than 8 g/t in each. Arithmetic mean of gold content for calc-silicate and skarn rocks from the quarry is $x_{n=6}$ = 4573.78 ppb (86.7–9210 ppb). In these rocks Au occurs as chemically bound gold in ore minerals, "visible" gold in form of microscopic inclusions in ore minerals, very fine grains in quartz ± calcite veinlets, or in tiny fissures in rock minerals. Calc-silicate rocks have a different composition of rock-forming minerals and are represented by pyroxene-garnet skarn or diopside ± tremolite ± calcite ± talc rocks, quartz-calcite rocks, and calc-serpentinite rocks.

Lower contents of gold were determined in leptynite gneisses and other rocks. Arithmetic mean of gold content in leptynite gneisses is $x_{n=5}$ = 430.42 ppb (3.9–1111 ppb). Highest Au content was detected in strongly silicificated leptynite sample cut by ore veinlets of arsenide and sulphide minerals from 1 up to 3 cm thick.

Arithmetic mean of gold content for all studied samples from the "Złoty Jar" quarry was almost 2 g/t for n = 18 (1.3–9210 ppb).

However, highest gold concentration (29 000 ppb) was determined in black serpentinites from old waste dumps of the Western Ore Field. This value and some other results of Au concentration in different rocks from the Western Ore Field are not marked on Figure 10b. Arithmetic mean of gold content for these samples was almost 3 g/t ($x_{n=23}$ = 2.8 ppm). Slightly lower Au concentrations from 1.4 up to 4.4 g/t were determined in samples of arsenic ore in calc-silicate rocks from old waste dumps of the Krzyżowa Mt. Ore Field.

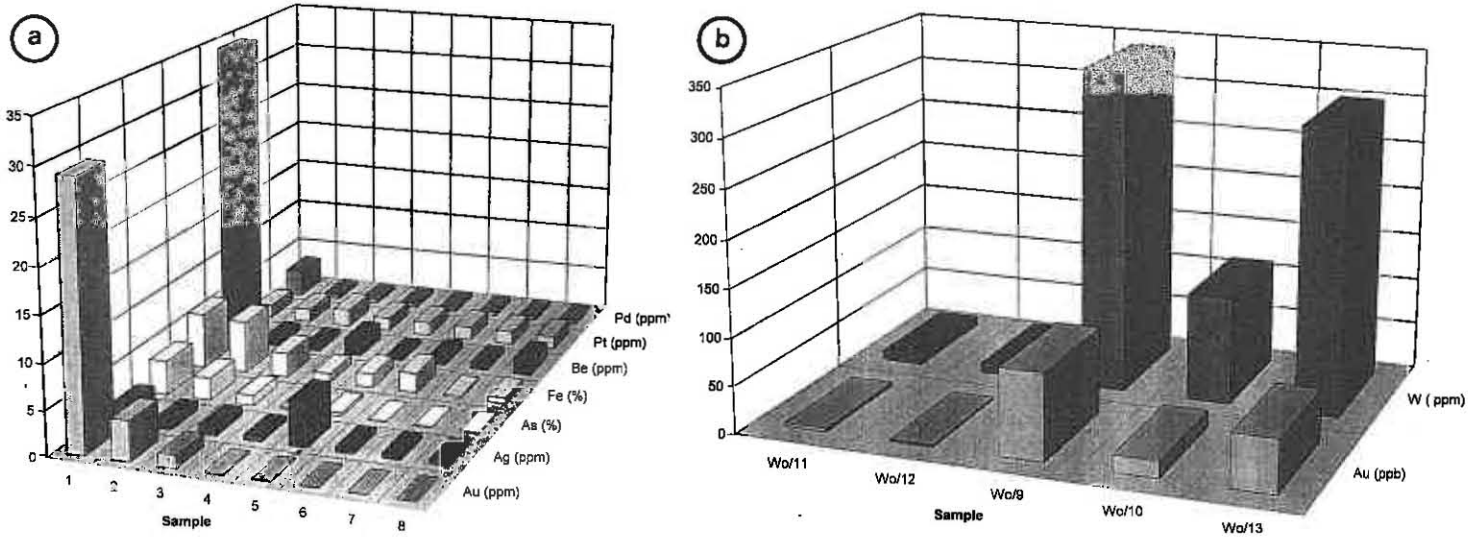

Fig. 11a, b. Histographs of element concentrations in rock samples: a — Au, Ag, As, Fe, Be, Pt and Pd content in rocks from old waste dump of the Western Ore Field; b — Au and W content in rocks from the "Złoty Jar" quarry
Histogramy zawartości pierwiastków w próbkach skał: a — Au, Ag, As, Fe, Be, Pt i Pd w skałach ze starych hałd kopalnianych Zachodniego Pola Rudnego; b — Au i W w skałach z kamieniołomu „Złoty Jar"

CHEMICAL RESULTS OF OTHER ELEMENT DETERMINATIONS

It is worth to present here, other results of element determination in calc-silicate rocks from the "Złoty Jar" quarry and in rocks from old waste dumps of the Western Ore Field (Fig. 11a, b). In black serpentinite sample, contained massive ores, the highest determined concentration of As was almost 4%, Au — 29 g/t, and over 35 ppm of Be. In the one sample of blastomylonitic amphibolite schist contained dense ore mineralization Pt (2 ppm) and Pd (3 ppm) were also determined.

Chemical results of W and Au presented here refers to calc-silicate rocks, skarn and leptynite gneisses from the "Złoty Jar" quarry. Samples were selected by use of U. V. lamp for the highest W content. Within them places with the highest visible scheelite mineralization (blue luminescence colour) have usually lower content of sulphides. Tungsten concentrations were from below 10 ppm (leptynites) up to 340 ppm (calc-silicate rocks). In Figure 11b are shown relations between W and Au in the same samples (max. 91 ppm and 56 ppb, respectively). Relatively high concentration of tungsten occurs in light green calc-silicate rocks which contains disseminated scheelite mineralization. Individual scheelite grains have sizes from 0.0X up to 1.X cm and in some places they formed spot-like concentration up to a few centimetres in size.

CONCLUSIONS

The exploitation of blastomylonitic schist for road construction use carried out in the "Złoty Jar" quarry, exposed narrow lenses of calc-silicate rocks, contained gold-bearing ore mineralization. These lenses are separated from old mining fields of the Złoty Stok As-Au mine by several faults. Origin of gold-bearing mineralization in the "Złoty Jar" quarry was a result of hydrothermal metasomatic processes developed in contact zone of the Kłodzko – Złoty Stok granitoid massif and within the regional shear-zone of post-Variscan time (Fig. 12). Although, in the "Złoty Jar" quarry a thicker zone of typical skarns (direct contact with granite is about 1.5 km apart) has not been developed. Nevertheless different metasomatic fronts carried various silicates along fractures allowed to form, at a smaller scale to compare to Western or Krzyżowa Mt. Ore Fields (W. M. Kowalski, 1963), gold-bearing calc-silicate rocks which in some narrow parts represent even poorly developed pyroxene and garnet skarns with gold-bearing ore minerals (**stage I**). The arsenides or sulphides are irregularly distributed in the calc-silicate rocks, and only in some local places formed small massive bodies. Especially enriched in gold-bearing ore minerals are zones developed in the primary contact of carbonate rocks with metavolcanites, which underwent strong alteration and supplied additional elements into metasomatic fluids. The dominant types of alteration are: silicification, carbonatization, serpentinization, sericitization, sulphidation, talcization, and prehnitization. All calc-silicate rocks in the quarry containing impregnated ore mineralization are cut by veinlets of a later paragenesis (quartz, calcite, adularia, amphiboles, green serpentine, prehnite, and others). Some of them contain ore mineralization and were developed as late stage cataclasis ores (**stage II** and **III**) according to the ductile-brittle and brittle deformational effects during development processes of the Złoty Stok – Trzebieszo-

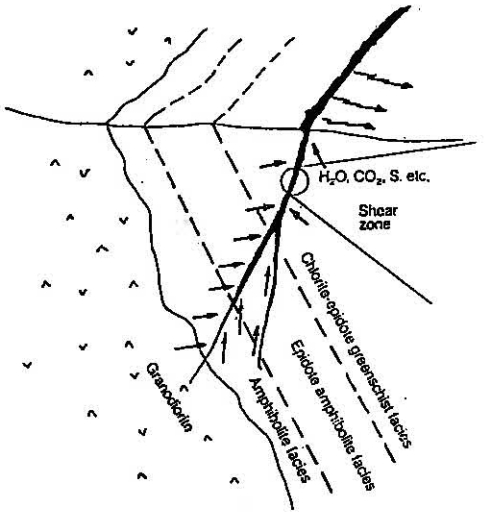

Fig. 12. Scheme of the general relation between metavolcanic rocks (greenstone), the granodiorite, the shear zones, wall-rock alteration in the shear zone, and the apparent movement directions of fluid (after R. W. Boyle, 1961)

Schemat ogólny relacji między skałami metawulkanicznymi (zieleńce), granodiorytem, strefami ścinań, przeobrażeniami metasomatycznymi skał w strefie ścinań i przypuszczalnymi kierunkami krążenia roztworów (według R. W. Boyle'a, 1961)

wice regional shear zone (ZSTSZ). Native gold and the rest of sulphides and ore minerals were found with these paragenesis.

Gold in the "Złoty Jar" quarry occur in two different forms:

a — in own phases as native gold, electrum;

b — as fine-dispersed isomorphic admixture in ore minerals.

The first form was documented during detailed microscopic studies in the forms of sub- and microscopic inclusion ("visible" gold) in (Ni, Fe, Co) sulphoarsenides, arsenopyrites, pyrites, as individual fine-grains in quartz ± calcite veinlets or in microfissures within rock forming minerals (e.g. diopside) in calc-silicate rocks. On the base of microprobe analyses three types of native gold are distinguished: electrum with content of Ag up to 31.6 wt. %, bismuth gold with Bi admixture up to 35 wt. % and "pure" native gold which sometimes contains up to 15 wt. % of Ag, Cu, As, and W. Most often the electrum in form of micro-inclusions (0.5–20 μm) in (Ni, Fe, Co) sulphoarsenides was observed. Within them an inclusion of bismuth gold was also found. Most purest native gold occurs in the form of individual fine grains in quartz veins which cutting calc-silicate rocks.

The second form of gold was determined with use microprobe analyse, as fine-dispersed admixture (so-called "invisible" gold) in: bismuthinite (up to 2.22 wt. % of Au), arsenopyrite (up to 1.4 wt. %), loellingite (up to 0.72 wt. %), (Ni, Fe, Co) sulphoarsenides (up to 0.4 wt. %).

Fine-dispersed gold occurring in ore minerals was syngenetic to associated high temperature mineralization in arsenopyrite and loellingite (stage I). Preliminary results of thermo-barometric studies of garnet, pyroxene, and scheelite from skarn and calc-silicate rocks, containing gold-bearing arsenopyrite and loellingite, indicated 464–480°C for real temperature of their crystallization and of pressure about 1.4 kbar from fluids with low salinity (4.9–5.2 wt. % NaCl equiv.). As a geological thermometer was used arsenopyrite of the I generation associated with loellingite in calc-silicate rocks. The arsenopyrites contain from 35.12 up to 36.72 at. % As, what may indicate for their crystallization in the temperature range from 420 up to 530°C.

Appearance of "visible" gold should be linked with younger stages (II, III) of hydrothermal fluids migration preceded by the following tectonic movements connected with development of the Złoty Stok – Trzebieszowice regional shear zone. In the considering area, fissures and voids within calc-silicate rocks were infilled by younger generations of ore minerals with "visible" gold inclusions or grains and numerous veins and veinlets of quartz ± scheelite ± calcite composition as well as adularia or phrenite ones. Preliminary results of thermo-barometric studies indicate for homogenization temperature of inclusion in quartz veinlets containing younger arsenopyrite-pyrite mineralization below 350°C (S. Z. Mikulski, 1995*b*). Presence of numerous inclusions of visible gold was connected with hydrothermal middle-, low-temperature mineral assemblages, represented mainly by (Ni, Fe, Co) sulphoarsenides associated with calcite and with As and Fe sulphides (stage III). Similar electrum-Fe-Co-Ni-As-S paragenesis was described in the mica schists from Przecznica region in the Kamienica Range (A. Piestrzyński *et al.*, 1992). Characteristic features this gold-bearing mineral association are: inhomogeneous chemical composition, locally zone structure of some sulphoarsenides crystals, and native gold (± native Bi) inclusions with different share of Ag (electrum, silver gold), Bi (bismuth gold) admixtures. Despite to observation presented by other geologists (A. Muszer, 1992; K. Niczyporuk, S. Speczik, 1993) described materials allow to propose an idea that native gold mineralization of this type in the earlier stages of crystallization are much pure and become progressively enriched in admixtures (silver > 30% Ag) with later remobilization.

Observed gold-bismuth myrmekites within sulphoarsenides in natural occurrences form as a result of solid solution decomposition of maldonite (Au_2Bi) in narrow margin within the high temperature range (P. Ramdohr, 1969). Common presence of Co-gersdorffite and Ni-cobaltite in carbonatized zones indicates Co, Ni and Fe remobilization processes from primary sulphoarsenides (arsenopyrite, cobaltite, gersdorffite) and their replacement and recrystallization in lower temperatures (stage III). Presumably, processes of Au, Ag, As, Ni, Co, Fe and other metals redistribution are more widespread in the Variscan hydrothermal systems of the Sudetes. Especially among mineralization associated with arsenic-polymetallic formation in Sudetes (S. Z. Mikulski, 1995*c*)

Other problems are native gold micrograins within fissures of ore minerals such as arsenopyrite, pyrite and loellingite. Gold remobilization process was occurring in a few stages. After primary deposition of invisible Au in solid-solution with oxide (?), sulphide and arsenide minerals began process of redistribution and concentration of solid-solution gold to form colloidal and microscopic particles in fractures and voids within the host minerals. Redistribution process of gold from arsenopyrite and loellingite started immediately after they formed (J. Heinhorst, B. Lehmann, 1994; P. Möller, G. Kersten, 1994; A. Mumin *et al.*, 1994). Further migration of Au, out of the host mineral and interstitial, to gangue minerals where the gold appears to have a long distance residence time (A. Mumin *et al.*, 1994). In the case of primary gold from the quarry redistribution of solid-solution Au and its concentration were observed in various stages. Gold-bearing rocks underwent a few tectonic stages during geological development. Arsenopyrite-loellingite association with pyrrhotite or magnetite evidence for reducing but moderately sulphide conditions of the ore formation. Gold has high solubility and mobility in the solutions from which crystallizations of sulphide-arsenic paragenesis are possible. The chloride complexes $AuCl_2^-$ and HS dominate in acid solutions at a temperature above 300°C. The hydrosulphide complex

$Au(HS)_2^-$ is a dominant species in the near-neutral to alkaline solutions (G. A. Pal'Yanowa, G. R. Kolonin, 1991; K. Hayashi, H. Ohmoto, 1991). The "visible" gold from the "Złoty Jar" quarry formed during several stages and processes of redistribution of primary gold from loellingite-arsenopyrite, magnetite(?) or pyrrhotite mineralization were wide developed and carried out by sulphur-bearing solutions at 350–250°C and near neutral — to alkaline environments with dominant role of hydrosulphide complex $Au(HS)_2^-$ in shear zones of brittle character.

Zakład Geologii Surowców Mineralnych
Państwowego Instytutu Geologicznego
Warszawa, Rakowiecka 4
Received:24.07.1996

REFERENCES

BAŁDYS L. (1954) — Dokumentacja złoża rudy arsenowej i złota w Złotym Stoku. Arch. Kopalni. Złoty Stok.

BANAŚ M. (1973) — Metallic mineralisation of Biała Góra near the Złoty Stok (in Polish with English summary). Spraw. z Pos. Komis. Nauk PAN Oddz. w Krakowie, **16**, p. 229–230, no. 1.

BORUCKI J. (1966) — Preliminary results of absolute age determination (K–A) of the Lower Silesian granitoidic rocks (in Polish with English summary). Kwart. Geol., **10**, p. 1–19, no. 1.

BOYLE R. W. (1961) — The geology, geochemistry, and origin of the gold deposits of the Yelowknife district. Geol. Surv. Can. Mem., **310**, p. 1–193.

BUDZYŃSKA H. (1971) — Mineralogy of arsenic deposits of the Złoty Stok (in Polish with English summary). Arch. Miner., **29**, p. 29–88, no. 1–2.

CASTROVIEJO R. (1990) — Gold ores related to shear zones, West Santa Comba-Fervenza Area (Galicia, NW Spain). Miner. Deposita, **25**, p. 42–52.

CWOJDZIŃSKI S.(1974) — Szczegółowa mapa geologiczna Sudetów, ark. Złoty Stok. Inst. Geol. Warszawa.

CWOJDZIŃSKI S. (1975) — On the origin and evolution of the northern part of the Złoty Stok – Skrzynka tectonic zone (in Polish with English summary). Kwart. Geol., **19**, p. 789–802, no. 4.

CYMERMAN Z. (1996) — The Złoty Stok-Trzebieszowice regional shear zone: the boundary of terranes in the Góry Złote Mts. (Sudetes). Geol. Quart., **40**, p. 89–118, no. 1.

DEPCIUCH T. (1972) — Absolute age of (K–Ar) granitoids from the Kłodzko – Złoty Stok area and the Niemcza zone (in Polish with English summary). Kwart. Geol., **16**, p. 103–112, no. 1.

DON J. (1964) — The Złote and Krowiarki Mts. as structural elements of the Śnieżnik metamorphic massif (in Polish with English summary). Geol. Sudetica, **1**, p. 79–114.

DZIEKOŃSKI T. (1972) — Wydobywanie i metalurgia kruszców na Dolnym Śląsku od XIII do XX w. Ossolineum. PAN.

FINCKH L., FISCHER G. (1938) — Geologische Karte von Preussen und benachbarten deutschen Ländern. Blatt Reichenstein. Berlin.

HAYASHI K., OHMOTO H. (1991) — Solubility of gold in NaCl-H_2S-bearing aquaeous at 250–350°C. Geochim. Cosmochim. Acta, **55**, p. 2111–2126.

HEINHORST J. P., LEHMANN B. (1994) — Electrochemical accumulation of visible gold on pyrite and arsenopyrite surfaces. Miner. Deposita, **29**, p. 399–403, no. 5.

JOHAN Z., MARCOUX E., BONNEMAISON E. M. (1989) — Arsénopyrite aurifére. Mode de substitution de Au dans la structure de FeAsS. C. R. Acad. Sc. Paris, **308**, p. 185–189. BRGM. Orléans.

KANASIEWICZ J. (1992) — Perspectives for finding the arsenical-gold-bearing mineralization joined with the Kłodzko – Złoty Stok granodioryte massif in the results of the geochemical monitoring (in Polish with English summary). Prz. Geol., **40**, p. 108–113, no. 2.

KLEMM D. (1965) — Synthesen und Analysen in den Dreiecksdiagrammen FeAsS-CoAsS-NiAsS und FeS_2-CoS_2-NiS_2. N. Jb. Miner. Abh., **103**, p. 205–225, no. 3.

KOWALSKI W. M. (1961) — The distribution of loellingite and sulphides in the arseno-gold bearing bed in the Złoty Stok in Lower Silesia (in Polish with English summary). Zesz. Nauk. AGH, Geologia, no. 4, p. 17–22.

KOWALSKI W. M. (1963) — Serpentynization in the arsenic ore deposit at Złoty Stok (Lower Silesia) (in Polish with English summary). Pr. Geol. Komis. Nauk Geol. PAN Oddz. w Krakowie, **12**, p. 55–76.

KOWALSKI W. M. (1969) — Ore minerals from Złoty Stok (Lower Silesia). New data on minerals occurring in Poland (I) (in Polish with English summary). Pr. Miner. Komis. Nauk Miner. PAN Oddz. w Krakowie, **16**, p. 23–42.

KOZŁOWSKA-KOCH M. (1973) — Polymetamorphites of the Złoty Stok — Skrzynka dislocation zone (in Polish with English summary). Geol. Sudetica, **8**, p. 121–155, no. 1.

KOZŁOWSKI A. (1995) — Sprawozdanie z wykonania badań inkluzji fluidalnych w próbkach scheelitonośnych. In: Badanie mineralizacji złota związanej z granitoidowym masywem kłodzko-złotostockim (ed. S. Z. Mikulski), p. 65–66.

KRETSCHMAR U., SCOTT S. D. (1976) — Phase relations involving arsenopyrite in the system Fe-As-S and their application. Can. Miner., **14**, p. 364–386.

LORENC M. W. (1995) — Role of basic magmas in the granitoid evolution (a comparative study of some Hercynian massifs) (in Polish with English summary). Geol. Sudetica, **28**, p. 3–113, no. 1.

MIKULSKI S. Z. (1994) — Mineralizacja scheelitowa i złotonośna w kamieniołomie w Złotym Jarze (Złoty Stok, Sudety). Pos. Nauk. Państw. Inst. Geol., **50** (2), p. 36–37.

MIKULSKI S. Z. (1995*a*) — Parageneza kwarcowo-scheelitowa w strefie wystąpień granitoidu kłodzko-złotostockiego. In: Góry Złote — geologia, okruszcowanie, ekologia (ed. A. Muszer), p. 57–63. Mat. Konf. Nauk. Wrocław – Złoty Stok 9–10.06.1995.

MIKULSKI S. Z. (1995*b*) — Badanie mineralizacji złota związanej z granitoidowym masywem kłodzko-złotostockim. Arch. Państw. Inst. Geol. Warszawa.

MIKULSKI S. Z. (1995*c*) — The arsenic-polymetallic gold bearing formations in the Sudetes — SW Poland. In: Promotion seminar "Tender for prospecting and exploration of gold in the Sudety Mts. and Fore-Sudetic Block" (ed. A. Wojciechowski), PGI, Warsaw 2.11.1995.

MIKULSKI S. Z. (in press) — Złoto z kamieniołomu Złoty Jar k/Złotego Stoku. Prz. Geol., **44**, no. 11.

MÖLLER P., KERSTEN G. (1994) — Electrochemical accumulation of visible gold on pyrite and arsenopyrite surfaces. Miner. Deposita, **29**, p. 404–413, no. 5.

MUMIN A., FLEET M., CHRYSSOULIS S. (1994) — Gold mineralization in As-rich mesothermal gold ores of the Bogosu-Prestea mining district of the Ashanti Gold Belt, Ghana: remobilization of invisible gold. Miner. Deposita, **29**, p. 445–460.

MUSZER A. (1992) — Native gold from the Złoty Stok deposit (Lower Silesia) (in Polish with English summary). Arch. Miner., **48**, p. 81–99.

MUSZER A. (1995) — Geneza okruszcowania skał w Górach Złotych. In: Góry Złote — geologia, okruszcowanie, ekologia (ed. A. Muszer), p. 52–56. Mat. Konf. Nauk. Wrocław – Złoty Stok 9–10.06.1995.

NEUHAUS A. (1933) — Die Arsen — Golderzlagerstätte von Reichenstein in Schlesien. Arch. Lagerst.-Forsch, **56**.

NICZYPORUK K., SPECZIK S. (1993) — Gold in arsenic minerals of Złoty Stok. Miner. Pol., **24**, p. 21–32, no. 1–2.

PAL'YANOWA G. A., KOLONIN G. R. (1991) — Physical-chemical model of transport and deposition of gold together with sulphides. In: Source, transport and deposition of metals, p. 693–696. Balkema. Rotterdam.

PIESTRZYŃSKI A., MOCHNACKA K., MAYER W., KUCHA H. (1992) — Native gold (electrum), Fe-Co-Ni arsenides and sulphoarsenides in the mica schists from Przecznica, the Kamienica Range, SW Poland. Miner. Pol., **23**, p. 27–42, no. 1.

QUIRING H. (1914) — Beiträge zur Kenntnis der niederschlesischen Goldvorkommen. Zeitscher. Pr. Geol., **22**. Berlin.

RAMDOHR P. (1969) — The ore minerals and their intergrowths. Pergamon Press. Oxford.

SAWICKI L. (1956) — Szczegółowa mapa geologiczna Sudetów, ark. Kamienica. Inst. Geol. Warszawa.

SHARP Z. D., ESSENE E. J., KELLY W. C. (1985) — A re-examination of the arsenopyrite geothermometer: pressure considerations and applications to natural assemblages. Can. Miner., **23**, p. 517–534.

SCHNEIDERHÖHN H. (1955) — Erzlagerstätten. III Aufl. Jena.

SMULIKOWSKI K. (1979) — Polymetamorphic evolution of the crystalline complex of the Śnieżnik and Góry Złote Mts. in the Sudetes (in Polish with English summary). Geol. Sudetica, **14**, p. 7–76, no. 1.

SPECZIK S. (1994) — Metasomatic processes in the vicinity of the Kłodzko-Złoty Stok massif. In: Second workshop on Variscan metallogeny Cracow – Wrocław – Warsaw, p. 85–101. Warsaw 18–29.07.1994.
WIENCKE O. (1907) — Über die Arsenerzlagerstätten von Reichenstein. Zeitscher. Pr. Geol., **15**. Berlin.
WIERZCHOŁOWSKI B. (1976) — Granitoids of the Kłodzko – Złoty Stok massif and their contact influence on the country rocks (petrographic characteristics) (in Polish with English summary). Geol. Sudetica, **11**, no. 2
WOJCIECHOWSKA I. (1975) — Tektonics of the Kłodzko – Złoty Stok granitoids massif and its country rocks in the light of mesostructural investigations (in Polish with English summary). Geol. Sudetica, **10**, p. 61–121, no. 2.
WOJCIECHOWSKA I. (1976) — Następstwo deformacji w polimetamorfitach okolic Złotego Stoku. In: Problemy wieku deformacji serii zmetamorfizowanych Ziemi Kłodzkiej, p. 106–114. Mat. Konf. Teren. Międzylesie 11–12.09.1976. Wrocław.
ŻABA J., BĘDKOWSKI Z. (1995) — Następstwo mezoskopowych stref ścinania w NE części metamorfiku Śnieżnika (na przykładzie polimetamorfitów z kamieniołomu Złoty Jar w Złotym Stoku). In: Góry Złote — geologia, okruszcowanie, ekologia (ed. A. Muszer), p. 20–27. Mat. Konf. Nauk. Wrocław – Złoty Stok 9–10.06.1995.

Stanisław Z. MIKULSKI

MINERALIZACJA ZŁOTONOŚNA W STREFIE METAMORFIZMU KONTAKTOWEGO I W STREFACH ŚCINAŃ W KAMIENIOŁOMIE „ZŁOTY JAR" — ZŁOŻE As-Au ZŁOTY STOK

Streszczenie

Złotonośne asocjacje mineralne w kamieniołomie „Złoty Jar" utworzyły się podczas trzech oddzielnych etapów. W etapie I — skarnopodobnego okruszcowania — miały miejsce procesy metasomatyczne metamorfizmu kontaktowego zachodzące w strefie egzokontaktowej kłodzko-złotostockiego masywu granodiorytowgo. Wstępne wyniki badań pierwotnych inkluzji fluidalnych wykazują, że najwcześniejszy etap krystalizacji piroksenu, granatu i scheelitu zachodził z roztworów o niskim zasoleniu (4,9–5,2% wag. równoważnika NaCl) w temperaturach 464–480° C i przy ciśnieniu poniżej 1.4 kbar. Z najmłodszymi fazami tego etapu związana jest najszerzej rozprzestrzeniona złotonośna mineralizacja löllingitowo-arsenopirytowa. Zdecydowana większość złota drobnodyspersyjnego występuje w postaci submikroskopowej wielkości drobin w minerałach kruszcowych nagromadzonych głównie w skałach węglanowo-krzemianowych i w czarnych serpentynitach (odpowiednio w stwierdzonych ilościach maksymalnych do 10 i 29 g/t). Młodsze złotonośne generacje kruszców (etapy II i III) wykazują formy, które pozwalają zaliczyć je do typowych mineralizacji rozwiniętych w strefach ścinań. Powstały one głównie wskutek wypełnień hydrotermalnych związanych z migracją roztworów minerałotwórczych w następstwie rozwoju kruchych stref ścinań. Temperatury homogenizacji pierwotnych inkluzji kwarcu żyłowego, zawierającego okruszcowanie i złoto "widzialne", wynoszą 220–280°C, przy zasoleniu 4–10% równoważnika NaCl. Złoto „widzialne" stwierdzono w formie wrostków o rozmiarach od 5 do 50 μm w siarkoarsenkach, siarczkach i w postaci pojedynczych mikroziarenek w żyłkach kwarcowych lub kwarcowo-kalcytowych. W najmłodszej opisanej złotonośnej asocjacji mineralnej w obrębie Ni-Fe-Co siarkoarsenków powszechnie obserwowano wrostki elektrum i myrmekitowe przerosty złota i bizmutu. Proces redystrybucji złota pierwotnego z minerałów arsenowo-löllingitowych na skalę lokalną i ze skał metawulkanicznych na skalę regionalną był szeroko rozprzestrzeniony. Wytrącanie złota „widzialnego" w obrębie młodszych asocjacji siarkoarsenków i siarczków zachodziło najprawdopodobniej przy udziale roztworów zawierających siarkę, w warunkach od obojętnych do zasadowych, w temperaturach poniżej 350°C i przy dominującej roli związków kompleksowych typu $Au(HS)_2^-$. Głównym źródłem metali były prawdopodobnie pre-waryscyjskie koncentracje metali w skałach wulkaniczno-osadowych (zawierających również elementy z górnego płaszcza — Pt, Pd), które uległy mobilizacji podczas formowania się intruzji granitoidowej. W arsenowo-złotonośnych nagromadzeniach widoczne są z kolei młodsze procesy redystrybucji metali spowodowane rozwojem stref ścinań.

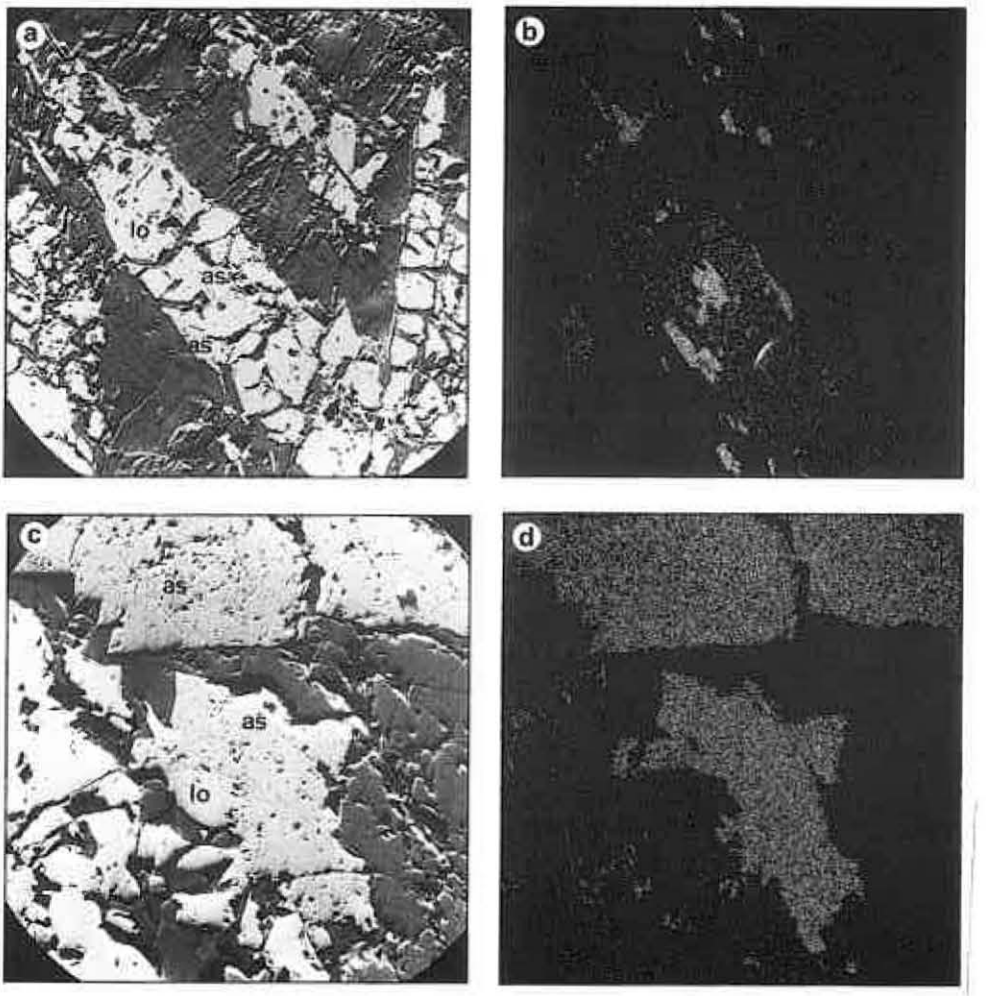

Fig. 13

Stanisław Z. MIKULSKI — Gold mineralization within contact-metamorphic, and shear zones in the "Złoty Jar" quarry — the Złoty Stok As-Au deposit area (Sudetes)

PLATE I

Fig.13a–d. Loellingite-arsenopyrite grain aggregates in calc-silicate rocks from the "Złoty Jar" quarry: a, c — backscatter electron images showing relationship between loellingite and arsenopyrite (lo — loellingite, as — arsenopyrite); b, d — distribution maps of characteristic SKα radiation; a, b — x 130, c, d — x 270

Agregaty ziarniste löllingitowo-arsenopirytowe w skałach węglanowo-krzemianowych z kamieniołomu „Złoty Jar": a, c — obraz BEI; widoczna relacja między löllingitem a arsenopirytem (lo — löllingit, as — arsenopiryt); b, d — mapy rozkładu promieniowania charakterystycznego SKα; a, b — 130 x, c, d — 270 x

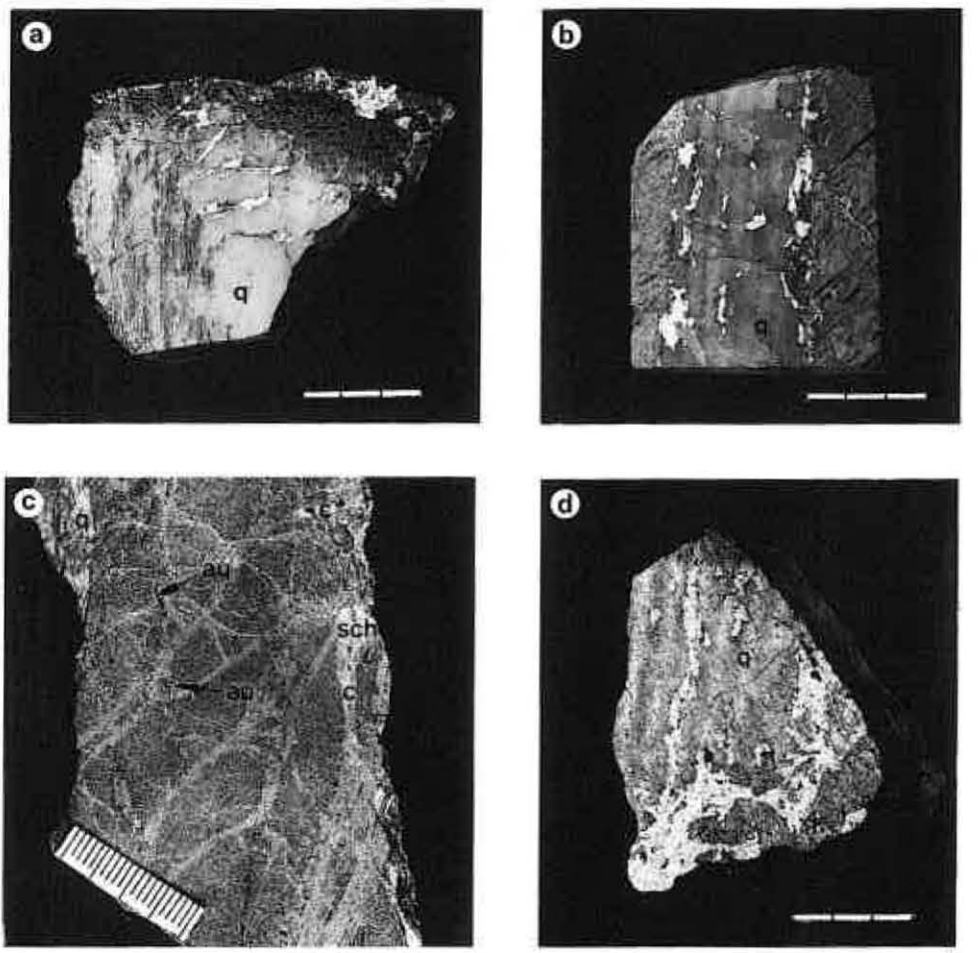

Fig. 14

Stanisław Z. MIKULSKI — Gold mineralization within contact-metamorphic, and shear zones in the "Złoty Jar" quarry — the Złoty Stok As-Au deposit area (Sudetes)

PLATE II

Fig. 14a–d. Textural relationships between arsenopyrite and gangue or host revealed textures which may contribute to a typological classification scheme of shear-zone gold ores: a — disseminated type, scale bar 4.5 cm; b, c — stringer or fine-banded type, scale bar 4.5 cm; d — massive ores type, scale bar 3 cm; white — arsenopyrite, q — quartz, c — calcite, sch — scheelite, au — native gold in Ni, Fe, Co sulphoarsenides; photo by J. Modrzejewska
Wzajemne relacje między formami wystąpień arsenopirytu (minerałów kruszcowych) i minerałów płonnych lub skały wskazują na tekstury, które można odnieść do typowych schematów klasyfikujących okruszcowanie w strefach ścinań: a — typ rozproszony, długość skali 4,5 cm; b, c — typ żyłkowy i wstęgowany drobno, długość skali 4,5 cm; d — typ masywny, długość skali 3 cm; biały — arsenopiryt, q — kwarc, c — kalcyt, sch — scheelit, au — złoto rodzime w Ni, Fe, Co-siarkoarsenkach; fot. J. Modrzejewska

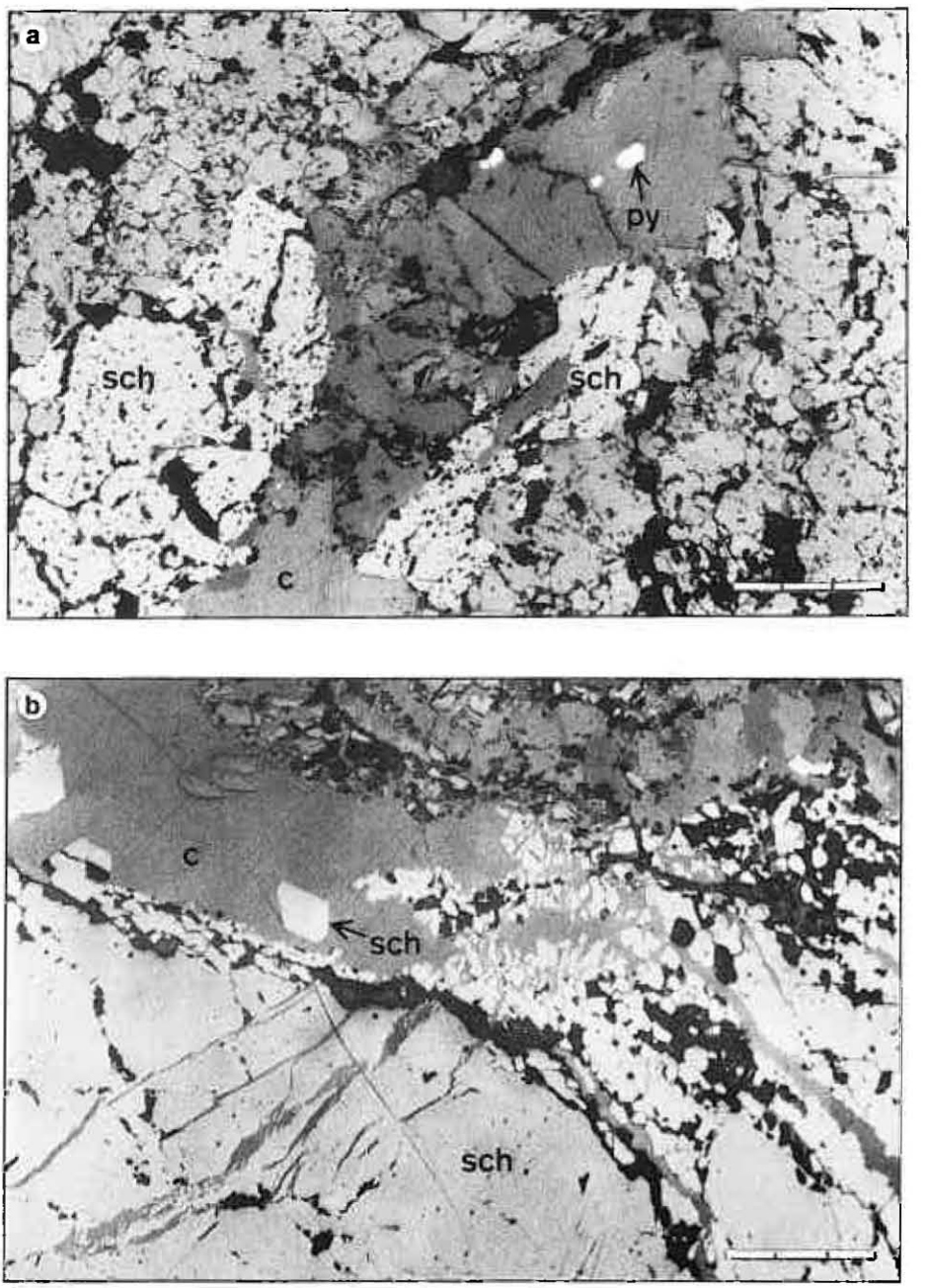

Fig. 15

Stanisław Z. MIKULSKI — Gold mineralization within contact-metamorphic, and shear zones in the "Złoty Jar" quarry — the Złoty Stok As-Au deposit area (Sudetes)

PLATE III

Fig. 15a, b. Scheelite mineralization in calc-silicate rocks: a — fractured scheelite coarse grain cuts calcite veinlet with pyrite; b — replacement of fractured scheelite by calcite; sch — scheelite, py — pyrite, c — calcite; scale bar 1 mm

Mineralizacja scheelitowa w skałach węglanowo-krzemianowych: a — spękane ziarno scheelitu przecięte młodszą żyłką kalcytową z pirytem; b — zastępowanie spękanego scheelitu kalcytem; sch — scheelit, py — piryt, c — kalcyt; długość skali 1 mm

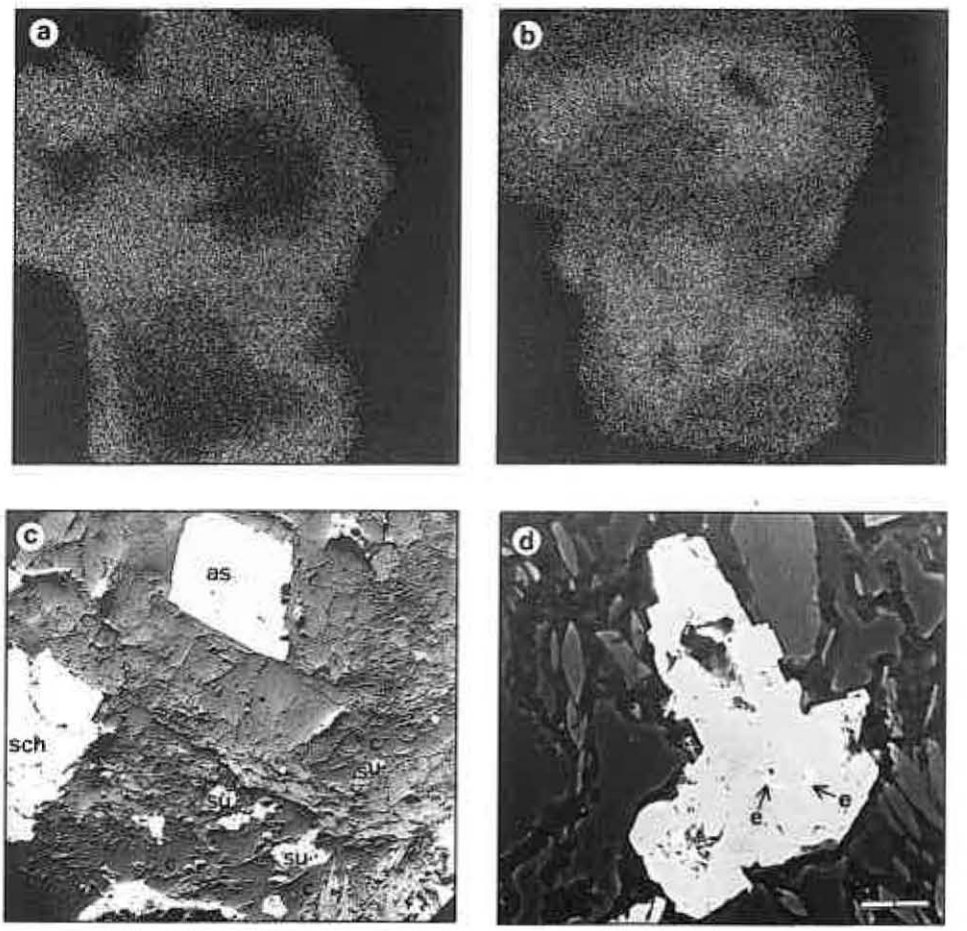

Fig. 16

Stanisław Z. MIKULSKI — Gold mineralization within contact-metamorphic, and shear zones in the "Złoty Jar" quarry — the Złoty Stok As-Au deposit area (Sudetes)

PLATE IV

Fig. 16a–d. Microprobe studies: a — distribution map of characteristic CoKα radiation; rims enriched in Co revealed composition of Ni-cobaltite; b — distribution map of characteristic NiKα radiation; cores enriched in Ni revealed composition of Co-gersdorffite; x 1600; c — backscatter electron images of ore mineralization (as — arsenopyrite, sch — scheelite, su — Ni-Fe-Co sulphoarsenides and sulphides, c — calcite), x 75; d — electrum (e) inclusions in Co-Ni sulphoarsenides grain, scale bar 10 μm

Badania w mikroobszarze: a — mapa rozkładu promieniowania charakterystycznego CoKα; strefa zewnętrzna wzbogacona w Co wykazuje skład Ni-kobaltynu; b — mapa rozkładu promieniowania charakterystycznego NiKα; strefa wewnętrzna wzbogacona w Ni wykazuje skład Co-gersdorffitu; 1600 x; c — obraz BEI mineralizacji kruszcowej (as — arsenopiryt, sch — scheelit, su — Ni-Fe-Co siarkoarsenki i siarczki, c — kalcyt), 75 x; d — wrostki elektrum (e) w siarkoarsenkach niklu i kobaltu, długość skali 10 μm

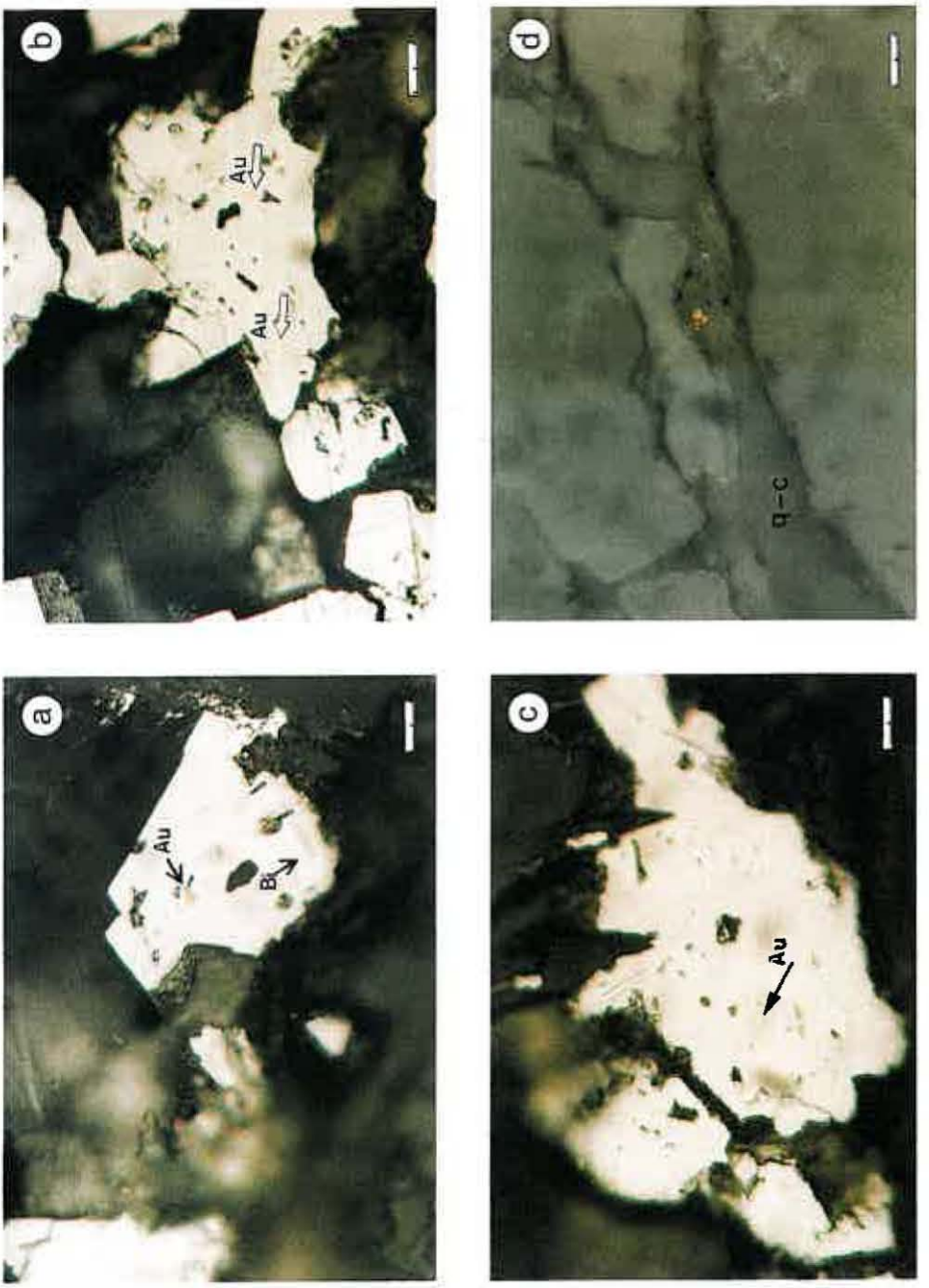

Fig. 17

Stanisław Z. MIKULSKI — Gold mineralization within contact-metamorphic, and shear zones in the "Złoty Jar" quarry — the Złoty Stok As-Au deposit area (Sudetes)

PLATE V

Fig. 17a–d. Native gold from the "Złoty Jar" quarry: a–c — native gold inclusions in Ni-Fe-Co sulphoarsenides (Au — gold, electrum, Bi — native bismuth), scale bar 20 μm; d — grain of native gold (yellow) in quartz-calcite veinlet (q–c) cuts calc-silicate rock, scale bar 100 μm

Złoto rodzime z kamieniołomu „Złoty Jar": a–c — wrostki złota rodzimego w siarkoarsenkach niklu, kobaltu i żelaza (Au — złoto, elektrum, Bi — bizmut rodzimy), długość skali 20 mm; d — ziarenko złota rodzimego (żółte) w żyłce kwarcowo-kalcytowej (q–c) wypełniającej spękanie w skale węglanowo-krzemianowej, długość skali 100 mm